

An ancestral recombination graph for diploid populations with skewed offspring distribution

Matthias Birkner¹, Jochen Blath², Bjarki Eldon^{2,*}

¹Institut für Mathematik, Johannes-Gutenberg-Universität Mainz, 55099 Mainz, Germany

²Institut für Mathematik, Technische Universität Berlin, 10623 Berlin, Germany

arXiv:1203.4950v2 [q-bio.PE] 30 Oct 2012

Running title:

An ancestral recombination graph admitting simultaneous multiple mergers

Keywords:

ancestral recombination graph, diploidy, skewed offspring distribution, simultaneous multiple merger coalescent processes, correlation in coalescence times, linkage disequilibrium, ratios of coalescence times.

Corresponding author:

Bjarki Eldon

Institute für Mathematik, Technische Universität Berlin, Strasse des 17. Juni 136, 10623 Berlin, Germany

office: +49 303 142 5762

eldon@math.tu-berlin.de

Abstract

A large offspring number diploid biparental multilocus population model of Moran type is our object of study. At each timestep, a pair of diploid individuals drawn uniformly at random contribute offspring to the population. The number of offspring can be large relative to the total population size. Similar ‘heavily skewed’ reproduction mechanisms have been considered by various authors recently, cf. e.g. Eldon and Wakeley (2006, 2008), and reviewed by Hedgecock and Pudovkin (2011). Each diploid parental individual contributes exactly one chromosome to each diploid offspring, and hence ancestral lineages can only coalesce when in distinct individuals. A separation of timescales phenomenon is thus observed. A result of Möhle (1998) is extended to obtain convergence of the ancestral process to an ancestral recombination graph necessarily admitting simultaneous multiple mergers of ancestral lineages. The usual ancestral recombination graph is obtained as a special case of our model when the parents contribute only one offspring to the population each time.

Due to diploidy and large offspring numbers, novel effects appear. For example, the marginal genealogy at each locus admits simultaneous multiple mergers in up to four groups, and different loci remain substantially correlated even as the recombination rate grows large. Thus, genealogies for loci far apart on the same chromosome remain correlated. Correlation in coalescence times for two loci is derived and shown to be a function of the coalescence parameters of our model. Extending the observations by Eldon and Wakeley (2008), predictions of linkage disequilibrium are shown to be functions of the reproduction parameters of our model, in addition to the recombination rate. Correlations in ratios of coalescence times between loci can be high, even when the recombination rate is high and sample size is large, in large offspring number populations, as suggested by simulations, hinting at how to distinguish between different population models.

Diploidy, in which each offspring receives two sets of chromosomes, one from each of two distinct diploid parents, is fairly common among natural populations. Mathematical models in population genetics tend to assume, however, that all individuals in a population are haploid, simplifying the mathematics. Mendel's Laws describe the mechanism of inheritance as composed of two main steps, equal segregation (First Law), and independent assortment (Second Law). The First Law proclaims gametes are haploid, i.e. carry only one of each pair of homologous chromosomes. Most models in population genetics are thus models of chromosomes, or gene copies. Mendel's Second Law proclaims independent assortment of alleles at different genes, or loci, into gametes. Linkage of alleles on chromosomes, resulting in non-random association of alleles at different loci into gametes, is of course an important exception to the Second Law.

Coalescent processes (KINGMAN, 1982a,b; HUDSON, 1983b; TAJIMA, 1983) describe the ancestral relations of chromosomes (or gene copies) drawn from a natural population. The coalescent was initially derived from a CANNINGS (1974) haploid exchangeable population model. Related ancestral processes take into account population structure (NOTOHARA, 1990; HERBOTS, 1997), selection (KRONE and NEUHAUSER, 1997; NEUHAUSER and KRONE, 1997; ETHERIDGE *et al.*, 2010), and recombination between linked loci (HUDSON, 1983a; GRIFFITHS, 1991; GRIFFITHS and MARJORAM, 1997). The coalescent has proved to be an important advance in theoretical population genetics, and a valuable tool for inference of evolutionary histories of populations.

Ancestral recombination graphs (ARG) (HUDSON, 1983a; GRIFFITHS, 1991; GRIFFITHS and MARJORAM, 1997) trace ancestral lineages of gene copies at linked loci, in which linkage is broken up by recombination. An ARG is a branching-coalescing graph, in which recombination leads to branching of ancestral chromosomes, and coalescence to segments rejoining. Coalescence events in an ARG may not lead to coalescence of gene copies at individual loci. An example ARG for two linked loci is given below, labelled as $ARG(1)$, with notation borrowed from DURRETT (2002). The labels a and b refer to the two alleles (types) at locus 1 and 2, respectively. A single chromosome with two linked alleles is denoted by (ab) , while chromosomes carrying ancestral alleles at only one locus are denoted (a) and (b) . When coalescence occurs at either locus, the number of alleles at the corresponding locus is reduced by one. The absorbing state, either (ab) or $(a)(b)$, is reached when alleles at both loci have coalesced.

$$\begin{aligned}
ARG(1) : \quad & (\mathbf{ab})(\mathbf{ab}) \xrightarrow{r} (\mathbf{a})(\mathbf{b})(\mathbf{ab}) \xrightarrow{c} (\mathbf{ab})(\mathbf{b}) \\
& \xrightarrow{r} (\mathbf{a})(\mathbf{b})(\mathbf{b}) \xrightarrow{c} (\mathbf{a})(\mathbf{b})
\end{aligned}$$

$$\begin{aligned}
ARG(2) : \quad & (\mathbf{ab})(\mathbf{ab}) \xrightarrow{r} (\mathbf{a})(\mathbf{b})(\mathbf{ab}) \xrightarrow{r} (\mathbf{a})(\mathbf{b})(\mathbf{a})(\mathbf{b}) \\
& \xrightarrow{c} (\mathbf{a})(\mathbf{b})
\end{aligned}$$

In $ARG(1)$, the first transition is a recombination, denoted by \xrightarrow{r} , followed by a coalescence (\xrightarrow{c}), in which the two alleles at locus 1 coalesce. Graph $ARG(1)$ serves to illustrate two important concepts we will be concerned with, namely correlation in coalescence times between alleles at different loci, and the restriction to binary mergers of ancestral lineages.

Correlation in coalescence times between types at different loci follows from linkage. Alleles at different loci can become associated due to a variety of factors, including changes in population size, natural selection, and population structure. Within-generation fecundity variance polymorphism induces correlation between a neutral locus and the locus associated with the fecundity variance (TAYLOR, 2009). Sweepstake-style reproduction (HEDGECKOCK *et al.*, 1982; HEDGECKOCK, 1994; BECKENBACH, 1994; AVISE *et al.*, 1988; PALUMBI and WILSON, 1990; ÁRNASON, 2004; HEDGECKOCK and PUDOVKIN, 2011), in which few individuals produce most of the offspring, has also been shown to induce correlation in coalescence times between loci (ELDON and WAKELEY, 2008). Understanding genome-wide correlations in coalescence times becomes ever more important as multi-loci genetic data becomes ubiquitous.

The ARG exemplified by $ARG(1)$ is characterised by admitting only binary mergers of ancestral lineages, i.e. exactly two lineages coalesce in each coalescence event. The restriction to binary mergers follows from bounds on the underlying offspring distribution, in which the probability of large offspring numbers becomes negligible in a large population (KINGMAN, 1982a,b). Sweepstake-style reproduction, in which few individuals contribute very many offspring to the population, have been suggested to explain the ‘shallow’ gene genealogy observed for many marine organisms (HEDGECKOCK *et al.*, 1982; HEDGECKOCK, 1994; AVISE *et al.*, 1988; PALUMBI and WILSON, 1990; BECKENBACH, 1994; ÁRNASON, 2004; HEDGECKOCK and PUDOVKIN, 2011). Large offspring number models are models of extremely high variance in individual reproductive output. Namely, individ-

uals can have very many offspring, or up to the order of the population size with non-negligible probability (SCHWEINSBERG, 2003; ELDON and WAKELEY, 2006; SARGSYAN and WAKELEY, 2008; SAGITOV, 2003; BIRKNER and BLATH, 2009). Such models do predict shallow gene genealogies, and can be shown to give better fit to genetic data obtained from Atlantic cod (ÁRNASON, 2004) than the Kingman coalescent (BIRKNER and BLATH, 2008; BIRKNER *et al.*, 2011; ELDON, 2011; STEINRÜCKEN *et al.*, 2012). Different large offspring number models will no doubt be appropriate for different populations, and the identification of large offspring number population models for each population is an open problem. For the sake of simplicity and mathematical tractability, the simple large offspring number model considered by ELDON and WAKELEY (2006) will be adapted to our situation.

The coalescent processes derived from large offspring number models belong to a large class of multiple merger coalescent processes introduced by DONNELLY and KURTZ (1999), PITMAN (1999), and SAGITOV (1999). Multiple merger coalescent processes (Λ -coalescents), as the name implies, admit multiple mergers of ancestral lineages in each coalescence event, in which any number of active ancestral lineages can coalesce, and at most one such merger occurs each time. In simultaneous multiple merger coalescent processes (MÖHLE and SAGITOV, 2001; SCHWEINSBERG, 2000a), any number of multiple mergers can occur each time, i.e. distinct groups of active ancestral lineages can coalesce each time. The ancestral recombination graph derived from our diploid large offspring number model admits simultaneous multiple mergers of ancestral lineages, as exemplified in $ARG(2)$. The last transition in $ARG(2)$ is a simultaneous multiple merger, in which the two types at each locus coalesce to separate ancestral chromosomes.

In order to investigate correlations in coalescence times among loci due to skewed offspring distribution, we *formally* derive an ancestral recombination graph, or a coalescent process for many linked loci, from our diploid large offspring number model. The key to the proof of convergence to an ancestral recombination graph from our diploid model lies in resolving the separation of timescales phenomenon we observe. Following Mendel’s Laws, the two chromosomes of an offspring come from distinct diploid parents. Chromosomes can therefore only coalesce when in distinct individuals. The ancestral process will consist of two phases, a dispersion phase occurring on a ‘fast’ timescale, and a coalescence and recombination phase occurring on a ‘slow’ timescale. In the dispersion phase, chromosomes paired together in diploid individuals disperse into distinct individuals. Coalescence

and recombination will only occur on the slow timescale. Similar separation of timescales issues arise in models of populations structured into infinitely many subpopulations (demes) (TAYLOR and VÉBER, 2009). When viewing the diploid individuals in our model as ‘demes’, our scenario departs from those describing structured populations by allowing only active ancestral lineages residing in *separate* ‘demes’ to coalesce. A simple extension of a result of MÖHLE (1998) yields convergence in our case.

The limiting process we formally obtain is an ancestral recombination graph for many loci admitting *simultaneous* multiple mergers of ancestral chromosomes (lineages). In simultaneous multiple merger coalescent processes, so-called Ξ -coalescents, different groups of active ancestral lineages can coalesce to different ancestors at the same time. Such coalescent processes were first studied as more abstract mathematical objects by SCHWEINSBERG (2000a), and derived from general single-locus population models by several authors (MÖHLE and SAGITOV, 2001; SAGITOV, 2003; SARGSYAN and WAKELEY, 2008; BIRKNER *et al.*, 2009). A Ξ -coalescent with necessarily up to quadruple simultaneous multiple mergers arises at each marginal locus (ie. considering each locus separately) in our model, since four parental chromosomes are involved in each reproduction event. This structure is intrinsically owed to our diploidy assumptions.

Formulas for the correlation in coalescence times between two alleles at two loci are obtained using our ancestral recombination graph (ARG). As predicted by J.E. Taylor (personal communication), these correlations will not necessarily be small even for loci separated by high recombination rate. This is a novel effect not visible in classical models. The correlation structure will of course depend on the underlying coalescent parameters introduced by the large offspring number model we adopt. An approximation of the expected value of the statistics r^2 , commonly used to quantify linkage disequilibrium, is also investigated using our ARG. In addition, we employ our ARG to investigate correlations in ratios of coalescence times between loci for samples larger than two at each locus, using simulations.

A diploid population model with multilocus recombination and skewed offspring distribution

The forward population model

Consider a population consisting of $N \in \mathbb{N} \equiv \{1, 2, \dots\}$ diploid individuals, meaning that each individual contains two *chromosomes*. Each chromosome is structured into $L \in \mathbb{N}$ loci. We assume

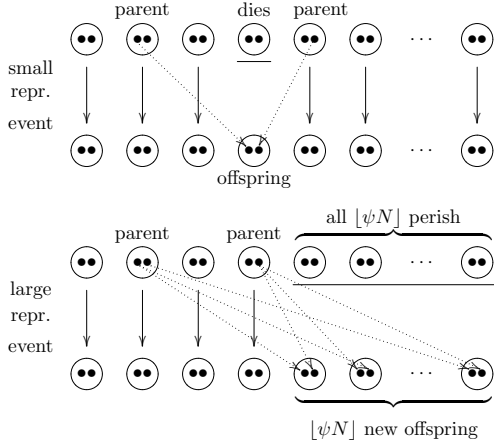


Figure 1: Illustration of ‘small’ and ‘large’ reproduction events without recombination. The dotted arrows indicate the copying of parental chromosomes into offspring chromosomes. The solid arrows indicate individuals that persist.

Moran-type dynamics: At each timestep (‘generation’), either a *small* or a *large* reproduction event occurs. In a *small* reproduction event, a single individual chosen uniformly at random from the population dies, and two other distinct individuals are chosen as *parents*. A diploid *offspring* is then formed by choosing one chromosome from each parent (see Figure 1). The parents always persist. A small reproduction event occurs with probability $1 - \varepsilon_N$, in which $\varepsilon_N \in (0, 1)$ depends on N . In a *large* reproduction event, a fraction $\psi \in (0, 1)$ of the population perishes, meaning that $\lfloor \psi N \rfloor$ individuals die ($\lfloor x \rfloor$ for $x \geq 0$ denotes the largest integer smaller than x). Two distinct individuals are then chosen uniformly from the remaining $N - \lfloor \psi N \rfloor$ individuals to act as parents of $\lfloor \psi N \rfloor$ offspring, and each offspring is formed independently by choosing one (potentially recombined) chromosome from each parent (see Figure 1). The population size always stays constant at N diploid individuals. Individuals that neither reproduce nor die simply persist.

Given the two parents, genetic types of the offspring individuals will then be obtained as follows. Each parent generates a large number of potential offspring chromosomes, of which a fraction $1 - r_N$ are exact copies of the original parental chromosomes, and a fraction r_N are *recombinants*. Each chromosome is structured into L loci. Recombination occurs only between loci, and never within. If recombination between a pair of chromosomes in a parent occurs between loci ℓ and $\ell+1 \in \{1, \dots, L\}$

(where we say that $X \in \{1, \dots, L-1\}$ is the *crossover point*), the two chromosomes exchange types at all loci from $\ell + 1$ to L . Only one crossover point is allowed in each recombination event. Let $r_N^{(\ell)}$ denote the probability of recombination between loci ℓ and $\ell + 1$ (i.e., the probability that the potential crossover point X equals ℓ). An offspring chromosome is a recombinant with probability $r_N = r_N^{(1)} + \dots + r_N^{(L-1)}$. Given that recombination happens, we thus have

$$\mathbb{P}\{X = \ell\} = \frac{r_N^{(\ell)}}{r_N^{(1)} + \dots + r_N^{(L-1)}}, \quad 1 \leq \ell \leq L - 1.$$

Each pair of recombined chromosomes is formed independently of all other pairs. From this large pool of chromosomes, each new offspring is randomly assigned (independently of all other offspring in the case of a large reproduction event), one potentially recombined chromosome generated by each parent. In addition, the reproduction mechanism in different generations is assumed to be independent.

Ancestral relationships - notation

Now we switch from the forward population model to its ancestral process, running backwards in time. Our sample will consist of $n \in \{1, \dots, 2N\}$ chromosomes, each subdivided into L loci. Hence, we need to keep track of the ancestry of nL segments (types/alleles). This implies that the different segments could end up on up to nL distinct chromosomes in nL distinct ancestral individuals. The required notation will now be introduced, and our discourse will therefore necessarily become a little bit technical. However, we believe that a precise description of the objects we are working with is essential. The key to understand our notation is that we are working with enumerated chromosomes, and ordered loci on chromosomes.

At present (that is, time step $m = 0$), assume that we consider an even number n of chromosomes carried by $n/2$ individuals. The chromosomes are enumerated from 1 to n , attaching consecutive numbers to chromosomes found in the same individual. Our ancestral process will keep track of the chromosomal ancestral information, that is, which locus is ancestral to which set of sampled chromosomes. That is, in each generation $m \in \mathbb{N}_0$ (backward in time), we will record all chromosomes which are *active* in the sense that they carry at least one locus which is ancestral to the same locus of at least one chromosome in generation 0. Denote the number of active chromosomes in generation $m \in \mathbb{N}_0$ by $\beta(m) \in \mathbb{N}$. The number $\beta(m)$ of active chromosomes can both increase, due to recombination, and decrease, due to coalescence, going back in time.

Now we explain our notation for the loci. For each chromosome $j \in [n] := \{1, \dots, n\}$, denote by $\mathbb{L}_\ell^{(j)}(m)$ locus $\ell \in [L]$ on chromosome j at time m . The subsets $\mathbb{L}_\ell^{(j)}(m)$ of $[n]$ contain all the numbers of chromosomes at present (time step 0) to which locus ℓ on active chromosome number j at time step m is *ancestral*. With this convention, and for each $m \in \mathbb{N}$ and $\ell \in [L]$, the collection

$$\{\mathbb{L}_\ell^{(j)}(m), j = 1, \dots, \beta(m)\}$$

which describes the configuration of segments (i.e. which have coalesced and which have not) at locus ℓ at time m , is a partition of $[n]$, i.e.

$$\mathbb{L}_\ell^{(j)}(m) \cap \mathbb{L}_\ell^{(\hat{j})}(m) = \emptyset \quad \text{for } j \neq \hat{j};$$

and

$$\bigcup_{j=1}^{\beta(m)} \mathbb{L}_\ell^{(j)}(m) = [n].$$

Thus, with our notation we can correctly describe the configuration of segments among chromosomes at any given time. By $C^{(j)}(m)$ we denote chromosome number j at time m . At time $m = 0$,

$$C^{(j)}(0) := \{\mathbb{L}_1^{(j)}(0), \dots, \mathbb{L}_L^{(j)}(0)\} := \{\{j\}, \dots, \{j\}\}.$$

For $m > 0$, consider the j -th active chromosome at generation m , where $j \in [\beta(m)]$. The corresponding ancestral information at generation m is encoded via an ordered list of subsets of $[n]$, setting

$$\begin{aligned} C^{(j)}(m) &:= \{\mathbb{L}_1^{(j)}(m), \dots, \mathbb{L}_L^{(j)}(m)\}, \\ \mathbb{L}_\ell^{(j)}(m) &\subset [n], \quad \ell \in [L]. \end{aligned} \tag{1}$$

Chromosomes are carried by diploid *individuals*. Keeping track of the grouping of active chromosomes into individuals will be important, since by our diploid reproduction mechanism, chromosomal lineages can only coalesce when in *distinct* individuals (see Example B below). In analogy with our previous nomenclature for our ancestral process, an *active* individual will carry at least one (and at most two) active chromosome(s). Let $b(m)$ denote the number of active individuals at generation

m where $\beta(m)/2 \leq b(m) \leq \beta(m)$ for all m . The ordered list of active chromosomes and the number of active individuals (called a ‘configuration’) at time $m \geq 0$ is denoted by

$$\xi^{n,N}(m) := \left\{ C^{(1)}(m), \dots, C^{(\beta(m))}(m); b(m) \right\}. \quad (2)$$

An individual number i at generation m is denoted by $\mathbb{I}_i(m)$, for $i \in [b(m)]$. An active individual is *single-marked*, if carrying one active chromosome, and is *double-marked*, if carrying two active chromosomes. Specifying the arrangement of chromosomes in individuals completes our description of the (prelimiting) ancestral process. However, since all active individuals are single-marked in the limiting process, our description of the arrangement of chromosomes in individuals is given in Section 1.1.1 in the Appendix. That is, each configuration $\xi^{n,N}(m)$ begins with the $2(\beta(m) - b(m))$ ordered consecutive chromosomes of the $\beta(m) - b(m)$ double marked individuals, followed by the $2b(m) - \beta(m)$ chromosomes contained in single-marked individuals. With this convention, the set of single- and double marked individuals and the grouping of chromosomes into individuals at generation m is uniquely determined by a configuration $\xi^{n,N}(m)$ of form (2). For notational convenience, the time index m will be omitted if there is no ambiguity.

For a given sample size n , the set of all possible ancestral configurations $\xi^{n,N}$ will be denoted by \mathcal{A}_n . The subset $\mathcal{A}_n^{\text{sm}} \subset \mathcal{A}_n$ of all configurations $\xi^{n,N} = \{C^{(1)}, \dots, C^{(\beta)}; b\}$ with $b = \beta$, i.e. configurations consisting only of single-marked individuals, will play an important rôle later on. Indeed, all configurations in the limiting model will be confined to the set $\mathcal{A}_n^{\text{sm}}$, and the pairing of chromosomes in individuals will become irrelevant.

The mapping cd (‘complete dispersion’)

$$\text{cd} : \mathcal{A}_n \rightarrow \mathcal{A}_n^{\text{sm}}$$

breaks up the pairing of chromosomes into diploid double-marked individuals. More precisely, we define

$$\text{cd} \left(\left\{ C^{(1)}, \dots, C^{(\beta)}; b \right\} \right) := \left\{ C^{(1)}, \dots, C^{(\beta)}; \beta \right\}. \quad (3)$$

Configurations in $\mathcal{A}_n^{\text{sm}}$ describe configurations in which all active individuals are single marked, i.e. carry only one active chromosome.

The effects of recombination and coalescence on the ancestral configurations in the case of two typical situations will now be illustrated. Example A will illustrate recombination, and Example B will illustrate coalescence of two chromosomes.

Example A. Suppose the most recent previous event in the history of a given configuration $\xi^{n,N}(m)$ was a *small reproduction event* (at time $m + 1$), and suppose that the resulting offspring individual is currently part of our configuration at time m , but neither of its parents is, and that the offspring individual is single-marked, i.e. carries one active chromosome. We obtain $\xi^{n,N}(m + 1)$ as follows:

- If there is no recombination during the reproduction event, then the configuration in the previous generation remains unchanged, i.e. $\xi^{n,N}(m + 1) = \xi^{n,N}(m)$.
- If there is recombination, say at a crossover point $X \in \{1, \dots, L - 1\}$, suppose the (single) offspring chromosome is

$$C^{(j)}(m) = \left\{ \mathbb{L}_1^{(j)}(m), \dots, \mathbb{L}_L^{(j)}(m) \right\}.$$

Necessarily, the two parental chromosomes will be part of the configuration $\xi^{n,N}(m + 1)$, residing in the same double-marked individual. More precisely, the two parental chromosomes, say $C^{(\bar{j})}(m + 1)$ and $C^{(\bar{j}+1)}(m + 1)$, are determined by (for $\ell \in [L]$)

$$\mathbb{L}_\ell^{(\bar{j})}(m + 1) = \begin{cases} \mathbb{L}_\ell^{(j)}(m) & : \quad 1 \leq \ell \leq X, \\ \emptyset & : \quad X + 1 \leq \ell \leq L, \end{cases}$$

and

$$\mathbb{L}_\ell^{(\bar{j}+1)}(m + 1) = \begin{cases} \emptyset & : \quad 1 \leq \ell \leq X, \\ \mathbb{L}_\ell^{(j)}(m) & : \quad X + 1 \leq \ell \leq L. \end{cases}$$

in which \emptyset denotes loci not carrying any ancestral segments. The offspring chromosome is of course not part of $\xi^{n,N}(m + 1)$. This transition can be partially trivial (a ‘silent recombination’ event), if the crossover point is not in an ‘active’ area, i.e. if $\mathbb{L}_\ell^{(j)} = \emptyset$ for $X + 1 \leq \ell \leq L$ (or for all $1 \leq \ell \leq X$). By way of example, with $L = 3$, if chromosome $C^{(j)} = \{ \{j\}, \{j\}, \{j\} \}$ was a recombinant, and the crossover point occurred between loci 2 and 3, the two parental chromosomes are given by $C^{(\bar{j})} = \{ \{j\}, \{j\}, \emptyset \}$ and $C^{(\bar{j}+1)} = \{ \emptyset, \emptyset, \{j\} \}$.

Example B. Suppose the most recent previous event in the history of a given configuration $\xi^{n,N}(m)$ of chromosomes at generation m is a *small reproduction event* at time $m + 1$, leading to a coalescence of lineages. This is the case e.g. if both a single-marked offspring individual with active chromosome $C^{\hat{j}}(m)$ is in our configuration $\xi^{n,N}(m)$, as well as its single marked parent (say with currently active chromosome $C^j(m)$), from which it actually obtained its active chromosome. Then, to obtain the configuration $\xi^{n,N}(m + 1)$, the offspring chromosome $C^{\hat{j}}(m)$ is deleted, and the resulting ancestral chromosome $C^{(j)}(m + 1)$ is given by the family of the union of the sets $\mathbb{L}_\ell^{(j)}$ and $\mathbb{L}_\ell^{(j)}$,

$$C^{(j)}(m + 1) = \left\{ \mathbb{L}_1^{(j)}(m) \cup \mathbb{L}_1^{(j)}(m), \dots, \mathbb{L}_L^{(j)}(m) \cup \mathbb{L}_L^{(j)}(m) \right\}. \quad (4)$$

All other chromosomes in $\xi^{n,N}(m+1)$ are copied from $\xi^{n,N}(m)$. Again, taking $L = 3$, if chromosomes $C^{(j)} = \{ \{j\}, \{j\}, \{j\} \}$ and $C^{(k)} = \{ \{k\}, \{k\}, \{k\} \}$ coalesce, the resulting ancestral chromosome is given by $C^{(j)} = \{ \{j, k\}, \{j, k\}, \{j, k\} \}$.

Scaling and classification of transitions

In order to obtain a non-trivial scaling limit for $\{\xi^{n,N}(m)\}$ as $N \rightarrow \infty$, the limit theorem of (MÖHLE and SAGITOV, 2001) (cf also the special case considered in (ELDON and WAKELEY, 2006)) suggests one should, for some constant $c > 0$, choose probability $1 - c/N^2$ for the small reproduction events, c/N^2 for the large reproduction events, i.e., setting

$$\varepsilon_N = c/N^2, \quad (5)$$

and speed up time by N^2 . For the recombination rate to be non-trivial in the limit (i.e. neither 0 nor infinitely large), we require that all recombination values $r_N^{(\cdot)}$ scale in units of N , i.e. for each crossover point $\ell \in [L] \setminus \{L\}$,

$$r_N^{(\ell)} := \frac{r^{(\ell)}}{N}, \quad 0 < r^{(\ell)} < \infty. \quad (6)$$

Thus, even though our timescale is in units of N^2 timesteps, recombination is scaled in units of N timesteps. On the level of single lineages the probability of recombination is of the order $O(N^{-2})$. Indeed, after a small reproduction event, the probability of drawing an offspring is $1/N$. The

probability that the offspring carries a recombined chromosome is of order $O(1/N)$.

Given the cornucopia of possible transitions from $\xi^{n,N}(m)$ to $\xi^{n,N}(m+1)$, it will be important to identify those transitions which are expected to be visible in the limiting process.

All possible transitions fall into the following three regimes:

- Those transitions which happen at probability of order $O(N^{-2})$ per generation, which will be visible in the limit (since time will be scaled by N^2). They will be called *effective transitions* and will appear at a finite positive rate in the limit.
- Further, there are transitions which happen less frequently, typically with probability of order $O(N^{-3})$ or smaller per generation, which will thus become negligible as $N \rightarrow \infty$ and hence be invisible in the limit. These will be called *negligible transitions*.
- Finally, there are transitions which happen much more frequently (with probability of order $O(N^{-1})$ or even $O(1)$ per generation). At first sight, one might think that their presence might lead to chaotic behaviour in the limit. However, this will not be case. Instead, these transition will happen ‘instantaneously’ in the limit, and result in a projection of the states of our process from \mathcal{A}_n into the subspace $\mathcal{A}_n^{\text{sm}}$, which will be the limiting statespace. This will be proved below. Such transitions will be called *projective* or *instantaneous* transitions. The identity transition is a special case of a projective transformation.

In the Appendix (section 1.1), a full classification of all transitions into the above groups is provided.

Instantaneous and effective transitions

The most important transitions and their effect for the limiting process will now be described in detail. Consider the following most recent events in the history of a set of lineages, i.e. events occurring at time $m+1$, from the perspective of the ancestral process $\xi^{n,N}(m)$ at time m :

- **Event 1 (silent):** A small reproduction event occurs, but the offspring is not active. This is the most likely event, and is of the order $O(1)$, but does not affect our ancestral configuration process $\xi^{n,N}(m)$, i.e. $\xi^{n,N}(m+1) = \xi^{n,N}(m)$. This event leads to an identity transition (a trivial *instantaneous transition*).

- **Event 2 (dispersion):** A small reproduction event occurs, the offspring is active in our sample but neither parent is, and recombination does not occur. This is a relatively frequent event which occurs with a probability of the order $O(N^{-1})$ per generation (since the probability that the offspring is in the sample is $b(m)/N$). If the offspring carries only one active chromosome, we again see an identity transition, i.e. $\xi^{n,N}(m+1) = \xi^{n,N}(m)$. If the offspring carries two active chromosomes, i.e. is a double-marked individual, the two active chromosomes will disperse to two separate individuals, who will then become single-marked individuals. Formally, for $\xi = \{C^{(1)}, \dots, C^{(\beta)}; b\} \in \mathcal{A}_n$ with at least one double-marked individual ($b < \beta$), define the map $\text{disp}_i(\cdot) : \mathcal{A}_n \rightarrow \mathcal{A}_n$ dispersing the chromosomes paired in individual i ,

$$\text{disp}_i(\xi) = \left\{ C^{(1)}, \dots, C^{(2i-2)}, C^{(2i+1)}, C^{(2i+2)}, \dots, C^{(2(\beta-b))}, C^{(2i-1)}, C^{(2i)}, C^{(2(\beta-b)+1)}, \dots, C^{(\beta)}; b+1 \right\} \quad (7)$$

if $1 \leq i \leq \beta - b$ and $\text{disp}_i(\xi) := \xi$ otherwise. Recall that the i -th double-marked individual has chromosomes labelled $2i - 1$ and $2i$. For $\xi^{n,N}(m)$, if the i -th double marked individual is affected, we have the transition $\xi^{n,N}(m+1) = \text{disp}_i(\xi^{n,N}(m))$.

The dispersion events will happen instantaneously as $N \rightarrow \infty$ (recall we are speeding time up by N^2), and thus will, in the limit, lead to an immediate complete dispersion of all chromosomes paired in double-marked individuals. If in the course of events, a new double-marked individual emerges due to pairing of active chromosomes in the same diploid individual, a dispersion of the chromosomes will occur immediately. **Event 2** will hence result in a permanent *instantaneous transition*, mapping our current state $\xi \in \mathcal{A}_n$ into the subspace $\mathcal{A}_n^{\text{sm}}$ by means of the map cd defined in (3). Our limiting process will thus live, with probability one for each given $t > 0$, in $\mathcal{A}_n^{\text{sm}}$, even if we start with a configuration from $\mathcal{A}_n \setminus \mathcal{A}_n^{\text{sm}}$ at time $t = 0$.

- **Event 3 (recombination):** A small reproduction event occurs, a single-marked offspring but neither parent is in our sample, and recombination affecting the active chromosome at a crossover point x . This event has probability of the order $O(N^{-2})$ per generation, and will thus be visible with finite positive rate in the limit. It is an *effective transition*, which can be described formally as follows. Define the recombination operation recomb acting on

chromosome j and crossover point x for a configuration $\xi \in \mathcal{A}_n^{\text{sm}}$ as

$$\text{recomb}_{j,x}(\xi) := \left\{ C^{(1)}, \dots, C^{(j-1)}, \tilde{C}^{(j,1)}, \right. \\ \left. \tilde{C}^{(j,2)}, C^{(j+1)}, \dots, C^{(\beta)}; \beta + 1 \right\}, \quad (8)$$

where

$$\tilde{C}^{(j,1)} = \left\{ \tilde{\mathbb{L}}_1^{(j,1)}, \dots, \tilde{\mathbb{L}}_L^{(j,1)} \right\}$$

with

$$\tilde{\mathbb{L}}_\ell^{(j,1)} = \begin{cases} \mathbb{L}_\ell^{(j)} & : \quad 1 \leq \ell \leq x - 1, \\ \emptyset & : \quad x \leq \ell \leq L, \end{cases}$$

and

$$\tilde{C}^{(j,2)} = \left\{ \tilde{\mathbb{L}}_1^{(j,2)}, \dots, \tilde{\mathbb{L}}_L^{(j,2)} \right\}$$

with

$$\tilde{\mathbb{L}}_\ell^{(j,2)} = \begin{cases} \emptyset & : \quad 1 \leq \ell \leq x - 1, \\ \mathbb{L}_\ell^{(j)} & : \quad x \leq \ell \leq L \end{cases}$$

(if one of $\tilde{C}^{(j,1)}$, $\tilde{C}^{(j,2)}$ equals $\{\emptyset, \dots, \emptyset\}$, we define $\text{recomb}_{j,\alpha}(\xi) := \xi$, giving rise to a *silent* recombination event).

- **Event 4 (pairwise coalescence):** A small reproduction event occurs, one single-marked parent and a single-marked offspring are in the sample, the active chromosome is inherited from the parent in the sample, and recombination does not occur. This event occurs with probability of order $O(N^{-2})$ and will therefore be visible in the limit with finite positive rate, hence gives rise to an *effective transition*. It will lead to a binary coalescence of lineages and can formally be described as follows. The ancestral chromosome $\tilde{C}^{(j_1)}$ formed by the coalescence of chromosomes j_1 and j_2 is given by

$$\tilde{C}^{(j_1)} = \left\{ \mathbb{L}_1^{(j_1)} \cup \mathbb{L}_1^{(j_2)}, \dots, \mathbb{L}_L^{(j_1)} \cup \mathbb{L}_L^{(j_2)} \right\} \quad (9)$$

if $1 \leq j_1 < j_2 \leq \beta$. Define the binary coalescence operation **pairmerge** acting on chromosomes

j_1 and j_2 ($1 \leq j_1 < j_2$) in a configuration $\xi \in \mathcal{A}_n^{\text{sm}}$ as

$$\text{pairmerge}_{j_1, j_2}(\xi) := \left\{ C^{(1)}, \dots, \tilde{C}^{(j_1)}, \dots, \right. \\ \left. C^{(j_2-1)}, C^{(j_2+1)}, \dots, C^{(\beta)}; \beta - 1 \right\} \quad (10)$$

if $1 \leq j_1 < j_2 \leq \beta$ (otherwise, we put $\text{pairmerge}_{j_1, j_2}(\xi) := \xi$).

- **Event 5 (multiple merger coalescence):** A large reproduction event occurs, neither parent but (possibly several) single marked offspring are in our sample, and recombination does not occur. This is again an event with probability of order $O(N^{-2})$ per generation and therefore will be visible in the limit with finite positive rate, hence gives rise to an *effective transition*. The offspring chromosomes will be assigned their parental chromosomes independently and uniformly at random, since due to an immediate ‘complete dispersion’ via **Event 2** each offspring individual will carry precisely one active chromosome. Now we formally define the multiple coalescence operation **groupmerge** for $\xi \in \mathcal{A}_n^{\text{sm}}$ and pairwise disjoint subsets $J_1, J_2, J_3, J_4 \subset [\beta]$ in which either at least one $|J_i| \geq 3$ or at least two of the $|J_i| \geq 2$. This transition is, thus, really different from a **pairmerge** transition. Let J_j denote the set of offspring chromosomes derived from parental chromosome j . Then

$$\text{groupmerge}_{J_1, J_2, J_3, J_4}(\xi) := \left\{ \tilde{C}^{(1)}, \tilde{C}^{(2)}, \tilde{C}^{(3)}, \right. \\ \left. \tilde{C}^{(4)}, C^{(j)}, j \in [\beta] \setminus (J_1 \cup J_2 \cup J_3 \cup J_4); \tilde{\beta} \right\} \quad (11)$$

with $((x)^+ := \max(x, 0))$

$$\tilde{\beta} = \beta - \sum_{j=1}^4 (|J_j| - 1)^+$$

and the four parental chromosomes, at least one of which is involved in a merger, are given by ($1 \leq i \leq 4$),

$$\tilde{C}^{(i)} = \left\{ \bigcup_{j \in J_i} \mathbb{L}_1^{(j)}, \dots, \bigcup_{j \in J_i} \mathbb{L}_L^{(j)} \right\}.$$

The chromosome(s) $C^{(j)}$ appearing in $\text{groupmerge}_{J_1, J_2, J_3, J_4}(\xi)$ denote the chromosomes in ξ that are not involved in a merger.

- **All other events:** Will either not affect our ancestral process, or have a probability of order smaller than N^{-2} so that they will be absent in the limit after rescaling. A complete classification of these events will be given in the Appendix (section 1.1).

The limiting dynamics and state space

The expected dynamics of the limiting continuous time Markov chain $\{\xi(t), t \geq 0\}$, taking values in \mathcal{A}_n , as $N \rightarrow \infty$, will now briefly be discussed.

- Complete dispersion (**Event 2**) of the sampled chromosomes is the first event to occur (between times $t = 0$ and $t = 0^+$). By \mathbb{I}_i we denote individual number i (see section 1.1.1 in Appendix). At time $t = 0$ when $\xi(0) \in \mathcal{A}_n$ we assume all n sampled chromosomes are paired in double-marked individuals (n even);

$$\xi(0) = \left\{ \mathbb{I}_i : \mathbb{I}_i = \left\{ C_0^{(2i-1)}, C_0^{(2i)} \right\}, \right. \\ \left. 1 \leq i \leq n/2 \right\}. \quad (12)$$

Immediately (at time 0^+), the chromosomes disperse into single-marked individuals,

$$\begin{aligned} \xi(0^+) &= \mathbf{cd}(\xi(0)) \\ &= \left\{ \mathbb{I}_i : \mathbb{I}_i = \left\{ C_0^{(i)}, \emptyset \right\}, 1 \leq i \leq n \right\} \\ &= \left\{ C_{0^+}^{(1)}, \dots, C_{0^+}^{(n)}; n \right\} \in \mathcal{A}_n^{\text{sm}}. \end{aligned} \quad (13)$$

- Throughout the evolution of the process, whenever double marked individuals appear (e.g. from a coalescence of lineages event), **Event 2** will immediately change our configuration to the corresponding ‘all dispersed’-configuration, i.e., for each $t > 0$,

$$\xi(t^+) = \mathbf{cd}(\xi(t)) \in \mathcal{A}_n^{\text{sm}}.$$

Such ‘flickering’ states will not affect any quantities of interest of our genealogy, so we can assume that they will be removed from the limit by choosing the càdlàg modification of $\{\xi(t), t \geq 0\}$, taking only values in $\mathcal{A}_n^{\text{sm}}$ for all $t > 0$ (this modification does not affect the finite-dimensional distributions of $\{\xi(t), t \geq 0\}$).

- Recombination (**Event 3**) appears in the limiting process at total rate $r = r^{(1)} + \dots + r^{(L-1)}$, where a certain recombination involving a given crossover point ℓ appears with rate $r^{(\ell)}$ on any lineage. Indeed, from our scaling considerations, we have for the probability of not seeing a recombination at ℓ in a small resampling event for more than $N^2 t$ scaled time units for a given single-marked individual satisfies $(r_N^{(\ell)} = r^{(\ell)}/N)$

$$\left(1 - \left(1 - \frac{c}{N^2}\right)r_N^{(\ell)}\frac{1}{N}\right)^{N^2 t} \rightarrow e^{-r^{(\ell)}t},$$

as $N \rightarrow \infty$ (recall (6); the probability for any given individual to be the child in a small reproduction event is $1/N$), hence the waiting time for this event to happen is exponential with rate $r^{(\ell)}$.

- Coalescences appear according to the effective transitions described by **Event 4** and **Event 5**. From the point of view of a given pair of active chromosomes in different individuals, a single pairwise coalescence will occur at rate $1 + c\frac{\psi^2}{4}C_{\beta;2;\beta-2}$ with $C_{\beta;2;\beta-2}$ from (15) (with $r = 1, s = \beta - 2$), where the 1 comes from a pairwise coalescence according to a small reproduction event, and the $c\frac{\psi^2}{4}C_{\beta;2;\beta-2}$ from a large merger event (the rates can be easily derived from considerations similar to the recombination rate r above), recalling that both coalescing chromosomes have to ‘successfully flip a ψ -coin’ in order to take part in the large coalescence event, and then are uniformly distributed into four groups according to the choice of any of the four potential parental chromosomes.

Given large coalescence events (involving at least three individuals, or at least two simultaneous pairwise mergers) happen with overall rate $c\frac{\psi^2}{4}$ times the corresponding coalescence rate of a Ξ -coalescent, obtained from the number of individuals taking part in the merger independently with probability ψ . The participating individuals are then being distributed uniformly into four groups according to the chosen parental chromosome. The corresponding rate is given in the third line of (14) (cf also (15)).

The limiting ancestral process

According to the above consideration, it is now plausible to consider the following limiting Markov chain as the ancestral limiting process. This fact will be proved below, with most computations provided in the Appendix. The m -th falling factorial is given by $(a)_m := a(a-1)\cdots(a-m+1)$,

$(a)_0 := 1$. The operations **pairmerge**, **recomb** and **groupmerge** for elements of $\mathcal{A}_n^{\text{sm}}$ were defined above in the section on scaling. Now we define the generator of the continuous-time ancestral recombination graph derived from our model.

Definition 1.1 (Limiting multilocus diploid ancestral recombination graph). *The continuous-time Markov chain $\{\xi(t), t \geq 0\}$ with values in $\mathcal{A}_n^{\text{sm}}$, initial condition $\xi(0) := \text{cd}(\xi)$ for $\xi \in \mathcal{A}_n$ and transition matrix G , with entries for elements $\xi', \xi \in \mathcal{A}_n^{\text{sm}}$, $\xi' \neq \xi$, is given by $(J := (J_1, \dots, J_4))$,*

$$G(\xi, \xi') = \begin{cases} 1 + c \frac{\psi^2}{4} C_{\beta; 2; \beta-2} & \text{if } \xi' = \text{pairmerge}_{j_1, j_2}(\xi) \\ r^{(\ell)} & \text{if } \xi' = \text{recomb}_{j, \ell}(\xi) \\ c \frac{\psi^2}{4} C_{\beta; |J|} & \text{if } \xi' = \text{groupmerge}_J(\xi) \\ 0 & \text{for all other } \xi' \neq \xi \end{cases} \quad (14)$$

(where in the penultimate line we only consider cases where either at least one $|J_i| \geq 3$ or at least two of the $|J_i| \geq 2$), with

$$C_{\beta; |J|} := C_{\beta; |J_1|, |J_2|, |J_3|, |J_4|; \beta - (|J_1| + |J_2| + |J_3| + |J_4|)}$$

and $(s = b - k_1 - \dots - k_r \geq 0, \quad x \wedge y := \min(x, y))$

$$C_{b; k_1, \dots, k_r; s} = \frac{4}{\psi^2} \sum_{l=0}^{s \wedge (4-r)} \binom{s}{l} \frac{(4)_{r+l}}{4^{k_1 + \dots + k_r + l}} \cdot (1 - \psi)^{s-l} (\psi)^{k_1 + \dots + k_r + l} \quad (15)$$

For the diagonal elements, one has of course

$$G(\xi, \xi) = - \sum_{\xi' \neq \xi, \xi' \in \mathcal{A}_n^{\text{sm}}} G(\xi, \xi'). \quad (16)$$

The rates in (15) are the transition rates of the Ξ -coalescent (a *simultaneous* multiple merger coalescent) with

$$\Xi = \delta_{(\psi/4, \psi/4, \psi/4, \psi/4, 0, 0, \dots)},$$

when r distinct groups of ancestral lineages merge. The number of lineages in each group is given by k_1, \dots, k_r , given β active ancestral lineages. The number $s = \beta - (k_1 + \dots + k_r) \geq 0$ gives the number of lineages (ancestral chromosomes) unaffected by the merger (cf. SCHWEINSBERG (2000a), Thm. 2). The particular form of Ξ given above follows from the fraction ψ of the population replaced by the offspring of the two parents in a large reproduction event, and our assumption that each parent contributes exactly one chromosome to each offspring. We have the following convergence result.

Theorem 1.2. *Let $\{\xi^{n,N}(m), m \geq 0\}$ be the ancestral process of a sample of n chromosomes in a population of size N and assume the scaling relations (5, 6). Then, starting from $\xi^{n,N}(0) \in \mathcal{A}_n$, we have that*

$$\{\xi^{n,N}(\lfloor N^2 t \rfloor)\} \rightarrow \{\xi(t)\}, \quad \text{as } N \rightarrow \infty,$$

in the sense of the finite-dimensional distributions on the interval $(0, \infty)$. The initial value of the limiting process is given by

$$\xi(0) = \text{cd}(\xi^{n,N}(0)) \in \mathcal{A}_n^{sm}.$$

A proof can be found in the Appendix. If $c = 0$, the classical ancestral recombination graph for a diploid population with recombination in the spirit of GRIFFITHS and MARJORAM (1997) results.

General diploid Moran-type models: “random” ψ

One of the aims of the present work is to understand the genome-wide correlations in gene genealogies induced by sweepstake-style reproduction. So far, we have discussed this for a very simple example of a sweepstake mechanism (analog to the one considered in ELDON and WAKELEY (2006)). More precisely, the fraction $\psi \in (0, 1)$ of the population replaced by the offspring of a single pair of individuals in a large offspring number event has hitherto been assumed to be (approximately) constant. Along the lines of the previous discussion, an ancestral recombination graph with a *randomized* offspring distribution can be derived (a comprehensive discussion of single-locus haploid Moran models in the domain of attraction of Λ -coalescents can be found in a recent article of HUILLET and MÖHLE (2011)). Even though ψ is now considered a random variable, the population size stays constant at N diploid individuals. Allowing ψ to be random may be biologically more realistic than taking ψ to be a constant. On the other hand, the problem of identifying suitable classes of probability distributions for ψ , reflecting the specific biology of given

natural populations, is still open and an area of active research.

To explain the convergence arguments when ψ is random, let the random variable Ψ_N , taking values in $[N - 2]$, denote the random number of diploid offspring contributed by the single reproducing pair of parents at each timestep; a new realisation of Ψ_N is drawn before each reproduction event. Again, we consider the effect of such a reproduction mechanism on coalescence events in a *sample*. The probability that two given chromosomes residing in two single-marked individuals in the sample coalesce in the previous timestep given the value of Ψ_N is

$$\begin{aligned} & \mathbb{P}(\{\text{pair coalescence}\} | \Psi_N = k) \\ &= \frac{1}{4} \delta_{\{k=1\}} \frac{4}{N(N-1)} \\ &+ \frac{1}{4} \delta_{\{k>1\}} \left(\frac{4k}{N(N-1)} + \frac{k(k-1)}{N(N-1)} \right), \end{aligned} \tag{17}$$

where the first and second terms on the right-hand side describe the case where one parent and one offspring are drawn, the third term covers the case where two offspring are drawn, and the 1/4 accounts for the probability that the two chromosomes in question must descend from the same parental chromosome. Define

$$c_N := 4\mathbb{P}(\{\text{pair coalescence}\}) \tag{18}$$

$$\begin{aligned} &= \sum_{k=1}^{N-2} \mathbb{P}(\{\text{pair coalescence}\} | \Psi_N = k) \mathbb{P}(\Psi_N = k) \\ &= \mathbb{E} \left[\frac{\Psi_N(\Psi_N + 3)}{N(N-1)} \right] \end{aligned} \tag{19}$$

(the factor 4 facilitates comparison with the haploid case). The sequence of laws $\mathcal{L}(\Psi_N)$, $N \in \mathbb{N}$, will be assumed to satisfy the following three conditions:

$$c_N \rightarrow 0 \quad \text{as } N \rightarrow \infty, \tag{20}$$

$$\begin{aligned} \frac{c_N}{\mathbb{E}[\Psi_N/N]} &= \frac{1/\mathbb{E}[\Psi_N/N]}{1/c_N} = \frac{\mathbb{E}[\Psi_N(\Psi_N + 3)]}{(N-1)\mathbb{E}[\Psi_N]} \\ &\rightarrow 0 \quad \text{as } N \rightarrow \infty, \end{aligned} \tag{21}$$

and there exists a probability measure F on $[0, 1]$ such that

$$\frac{1}{c_N} \mathbb{P}(\Psi_N > Nx) \xrightarrow{N \rightarrow \infty} \int_x^1 \frac{1}{y^2} F(dy) \quad (22)$$

for all continuity points $x \in (0, 1]$ of F .

Condition (20) is necessary for any limit process of the genealogies to be a continuous-time Markov chain, condition (21) ensures that a separation of time scales phenomenon occurs, and (22) fixes the limit dynamics of the large merging events (it is analogous to (SAGITOV, 1999, necessary condition (13)) in the haploid case). In the proof of convergence to a limit process we will recall equivalent conditions to (22) (see Appendix, section 1.4). Condition (20) implies (see Section 1.4 in Appendix)

$$\mathbb{E}[\Psi_N/N] \rightarrow 0 \quad \text{as } N \rightarrow \infty, \quad (23)$$

i.e. the probability for a given individual to be an offspring in a given reproduction event becomes small. Hence, (23) and (21) together show that there will be two diverging time-scales: The “short” time-scale $1/\mathbb{E}[\Psi_N/N]$ on which chromosomes paired in double-marked individuals disperse into single-marked individuals and the “long” time-scale $1/c_N$ over which we observe non-trivial ancestral coalescences.

In order to obtain a non-trivial genealogical limit process, we will then speed up time by a factor of $4/c_N$, i.e., $4/c_N$ reproduction events correspond to one coalescent time unit (see Thm. 1.3 below). This time rescaling is chosen in order for two chromosomes to coalesce at rate 1 in the limit. The required scaling relation for the recombination rates is now

$$r_N^{(\ell)} \sim \frac{c_N}{4\mathbb{E}[\Psi_N/N]} r^{(\ell)} \quad \text{as } N \rightarrow \infty \quad (24)$$

with $r^{(\ell)} \in [0, \infty)$ fixed for $\ell = 1, \dots, L - 1$ (where $f(N) \sim g(N)$ means $\lim_{N \rightarrow \infty} f(N)/g(N) = 1$). An intuitive explanation for the requirement (24) is that since the probability for a given individual to be an offspring in a given reproduction event is $\mathbb{E}[\Psi_N/N]$, after speeding up time by $4/c_N$, on any lineage recombination events between locus ℓ and $\ell + 1$ occur as a Poisson process with rate $r^{(\ell)}$.

A simple sufficient condition for (21) is the following: For any $\varepsilon > 0$,

$$N\mathbb{P}(\Psi_N > \varepsilon N) \rightarrow 0 \quad \text{as } N \rightarrow \infty. \quad (25)$$

Indeed, we have, by assuming $N > \varepsilon N$,

$$\begin{aligned} \mathbb{E}[\Psi_N^2] &= \sum_{k=1}^{\lfloor \varepsilon N \rfloor} k^2 \mathbb{P}(\Psi_N = k) + \sum_{k=\lfloor \varepsilon N \rfloor + 1}^N k^2 \mathbb{P}(\Psi_N = k) \\ &\leq \sum_{k=1}^{\lfloor \varepsilon N \rfloor} k \varepsilon N \mathbb{P}(\Psi_N = k) + \sum_{k=\lfloor \varepsilon N \rfloor + 1}^N N^2 \mathbb{P}(\Psi_N = k) \\ &\leq \varepsilon N \mathbb{E}[\Psi_N] + N^2 \mathbb{P}(\Psi_N > \varepsilon N). \end{aligned}$$

Dividing by $N\mathbb{E}[\Psi_N]$ gives

$$\frac{\mathbb{E}[\Psi_N^2]}{N\mathbb{E}[\Psi_N]} \leq \varepsilon + \frac{N\mathbb{P}(\Psi_N > \varepsilon N)}{\mathbb{E}[\Psi_N]},$$

and, since $\mathbb{E}[\Psi_N] > 1$,

$$\limsup_{N \rightarrow \infty} \frac{\mathbb{E}[\Psi_N^2]}{N\mathbb{E}[\Psi_N]} < \varepsilon + \limsup_{N \rightarrow \infty} N\mathbb{P}(\Psi_N > \varepsilon N) = \varepsilon.$$

Thus, condition (21) is obtained since we can choose ε to be as small as we like.

The limiting genealogical process will then be a continuous-time Markov chain on $\mathcal{A}_n^{\text{sm}}$ with generator matrix G whose off-diagonal elements are given by (for the values on the diagonal we again have (16))

$$G(\xi, \xi') = \begin{cases} C_{\beta;2} & \text{if } \xi' = \text{pairmerge}_{j_1, j_2}(\xi) \\ r^{(\ell)} & \text{if } \xi' = \text{recomb}_{j, \ell}(\xi) \\ C_{\beta;|J|} & \text{if } \xi' = \text{groupmerge}_{J_1, J_2, J_3, J_4}(\xi) \\ 0 & \text{for all other } \xi' \neq \xi \end{cases} \quad (26)$$

where

$$C_{\beta;|J|} := C_{\beta;|J_1|, |J_2|, |J_3|, |J_4|; \beta - (|J_1| + |J_2| + |J_3| + |J_4|)},$$

$k = (k_1, \dots, k_r)$, $|k| = k_1 + \dots + k_r$, and

$$\begin{aligned}
C_{b;k;s} &= 4 \sum_{l=0}^{s \wedge (4-r)} \binom{s}{l} \frac{(4)_{r+l}}{4^{|k|+l}} \\
&\cdot \int_{[0,1]} x^{|k|+l} (1-x)^{s-l} \frac{1}{x^2} F(dx) \\
&= F(\{0\}) \delta_{\{r=1, k_1=2\}} \\
&+ 4 \sum_{l=0}^{s \wedge (4-r)} \binom{s}{l} \frac{(4)_{r+l}}{4^{|k|+l}} \\
&\cdot \int_{(0,1]} x^{|k|+l} (1-x)^{s-l} \frac{1}{x^2} F(dx) \tag{27}
\end{aligned}$$

with F from (22). As in the case of constant ψ , the third line in (26) gives the transition rates for a given merger into r (≤ 4) groups of sizes k_1, \dots, k_r when β active ancestral lineages are present, with $s = \beta - |k| \geq 0$ lineages unaffected by a given merger of the Ξ -coalescent with

$$\Xi = \int_{[0,1]} \delta_{(x/4, x/4, x/4, x/4, 0, \dots)} F(dx),$$

(cf. SCHWEINSBERG (2000a), Thm. 2). By way of example, $C_{2;2;0} = 1$. Now we can state the convergence of our ancestral recombination graph process with random ψ . The analogue of Theorem 1.2 is the following:

Theorem 1.3. *Let $\{\xi^{n,N}(m), m \geq 0\}$ be the ancestral process of a sample of n chromosomes in a population of size N with offspring laws $\mathcal{L}(\Psi_N)$ which satisfy (20), (21) and (22), and assume the scaling relation (24) for the recombination rates. Then, starting from $\xi^{n,N}(0) \in \mathcal{A}_n$, we have that*

$$\{\xi^{n,N}(\lfloor 4t/c_N \rfloor)\} \rightarrow \{\xi(t)\}, \quad \text{as } N \rightarrow \infty,$$

in the sense of the finite-dimensional distributions on the interval $(0, \infty)$. The process $\{\xi(t)\}$ is the Markov chain with generator matrix (26) and initial value $\xi(0)$ given by

$$\xi(0) = \text{cd}(\xi^{n,N}(0)) \in \mathcal{A}_n^{sm}.$$

The proof is given in Section 1.4 in Appendix.

While $c_N \geq 1/N^2$ by definition, in principle any decay behaviour of c_N that is consistent with $\liminf_{N \rightarrow \infty} N^2 c_N \geq 1$, and hence any therefrom derived scaling relation between coalescent time scale and model census population size, is possible via a suitable choice of the family $\mathcal{L}(\Psi_N)$, $N \in \mathbb{N}$.

For an extreme example, let $\Psi_N \equiv \lfloor N^\gamma \rfloor$ for some $\gamma \in (0, 1)$, then $c_N \sim N^{-2(1-\gamma)}$ and (22) is satisfied with $F = \delta_0$.

The relation with the ‘‘fixed ψ ’’ model is as follows: For Theorem 1.2, we used the simple mixture distribution for Ψ_N :

$$\mathbb{P}(\Psi_N = \lfloor \psi N \rfloor) = 1 - \mathbb{P}(\Psi_N = 1) = \frac{c}{N^2} \quad (28)$$

for Ψ_N , in which $\psi \in (0, 1)$ and $c > 0$ are both constants. Our choice (28) of law for Ψ_N gives, using (17),

$$\begin{aligned} c_N &= \mathbb{E} \left[\frac{\Psi_N(\Psi_N + 3)}{N(N-1)} \right] \\ &= \left(1 - \frac{c}{N^2}\right) \frac{4}{N(N-1)} + \frac{c}{N^2} \frac{\psi N(\psi N + 3)}{N(N-1)} \\ &\sim \frac{1}{N^2} (4 + c\psi^2). \end{aligned}$$

Define $1_{(0,\psi)}(x) = 1$ if $x \in (0, \psi)$, and $1_{(0,\psi)}(x) = 0$ otherwise. Our choice (28) further gives

$$\begin{aligned} \mathbb{P}(\Psi_N > Nx) &= 1_{(0,\psi)}(x) \mathbb{P}(\Psi_N > Nx) \\ &= 1_{(0,\psi)}(x) cN^{-2}, \end{aligned}$$

and therefore

$$\begin{aligned} \frac{1}{c_N} \mathbb{P}(\Psi_N > \lfloor Nx \rfloor) &\longrightarrow 1_{(0,\psi)}(x) \frac{c}{4 + c\psi^2} \\ &= \int_{(x,1]} y^{-2} F(dy) \end{aligned}$$

with

$$F = \frac{4}{4+c\psi^2} \delta_0 + \frac{c\psi^2}{4+c\psi^2} \delta_\psi.$$

Furthermore, $\mathbb{E}[\Psi_N/N] = 1/N + O(1/N^2)$, thus

$$\frac{c_N}{4\mathbb{E}[\Psi_N/N]} \sim \frac{1}{N} \frac{4 + c\psi^2}{4}$$

and Theorem 1.2 follows from Theorem 1.3 (after rescaling time in the limit process $\{\xi(t)\}$ by a factor of $(4 + c\psi^2)/4$).

The constant $C_{b;k} := C_{b;k_1, \dots, k_r; s}$ (27) depends on the probability measure F . The form of F will no doubt be different for different populations. We reiterate that resolving the mechanism of sweepstake-style reproduction will require detailed knowledge of the reproductive behaviour and the ecology of the organism in question, along with comparison of model predictions to multi-loci genetic data. A candidate for F may be the beta distribution with parameters $\vartheta > 0$ and $\gamma > 0$, in which case the constant $C_{b;k}$ in (26) takes the form ($|k| := k_1 + \dots + k_r$)

$$C_{b;k} = 4 \sum_{\ell} \binom{s}{\ell} (4)_{r+\ell} \left(\frac{1}{4}\right)^{|k|+\ell} \cdot \frac{B(|k| + \ell + \vartheta - 2, s + \gamma - \ell)}{B(\vartheta, \gamma)}, \quad (29)$$

$B(\cdot, \cdot)$ being the Beta function.

Different scaling regimes

The mechanism of sweepstake-style reproduction may be different for different populations, and the frequency of large offspring number events may also be different. The particular timescale of the large reproduction events (we chose $\varepsilon_N = c/N^2$) results in a separation of timescales of the limit process. Resolving the separation of timescales problem results in the ARG with generator (14). Different scalings of ε_N result in different limit processes. By way of example, if $N^2\varepsilon_N \rightarrow 0$, large offspring number events are negligible in a large population, and we obtain the ARG associated with the usual Wright-Fisher reproduction, which can be read off Equation (14) by taking $c = 0$. One other scaling regime may seem reasonable, namely taking large offspring number events to be more frequent than in Assumption (5), but not too frequent. In mathematical notation, $N^2\varepsilon_N \rightarrow \infty$ and $N\varepsilon_N \rightarrow 0$. The ancestral process in this regime is again characterised by instantaneous separation of marked chromosomes into single-marked individuals, followed by coalescence and recombination occurring on the slow timescale. The probability of recombination is proportional to $N\varepsilon_N$ since the slow timescale must be in units proportional to $1/\varepsilon_N$. Hence, small reproduction events become

negligible in the limit, and the generator of the limit process is given by

$$G(\xi, \xi') = \begin{cases} \frac{\psi^2}{4} C_{\beta;2;\beta-2} & \text{if } \xi' = \text{pairmerge}_{j_1, j_2}(\xi) \\ r^{(\ell)}/r & \text{if } \xi' = \text{recomb}_{j, \alpha}(\xi) \\ \frac{\psi^2}{4} C_{\beta;|J|} & \text{if } \xi' = \text{groupmerge}_J(\xi) \\ 0 & \text{for all other } \xi' \neq \xi \end{cases} \quad (30)$$

in which $C_{\cdot, \cdot, \cdot}$ is given by Equation (15). The requirement $N\varepsilon_N \rightarrow 0$ is needed to prevent unreasonably high rate of recombination.

Haploid analogs

A haploid version of the above model, where only one parent contributes offspring at each timestep, is a specific example of a Λ -coalescent, where

$$\Lambda(dx) = \delta_0(dx) + c\psi^2\delta_\psi(dx), \quad \psi \in (0, 1), \quad c \in [0, \infty),$$

see e.g. ELDON and WAKELEY (2006) and BIRKNER and BLATH (2009). More precisely, as the population size N tends to infinity, assume probability $1 - c/N^2$ for the small reproduction events, c/N^2 for the large reproduction events (i.e., choose $\varepsilon_N = c/N^2$), and speed up generation time by N^2 . Again, by randomising ψ and/or switching to different scaling regimes, it is possible to obtain any given Λ -coalescent as limiting genealogy.

Two-sex extensions

Recent studies of the spawning behaviour of Atlantic cod indicate that cod adopts a lekking behaviour, in which males compete for females, and females exercise mate choice (NORDEIDE and FOLSTAD, 2000). Direct microsatellite DNA analysis indicates that although multiple paternity is sometimes detected, the reproductive success is highly skewed among the males, i.e. most of the successfully fertilized eggs can be attributed to a single male (HUTCHINGS *et al.*, 1999). Our model thus seems a good approximation to the actual reproduction mechanism of cod. Modifications to allow two distinct genders, and multiple paternity, are in principle straightforward.

More general recombination models

Our model can easily be enriched to allow also more general recombination events involving more than one crossover point at a time. Furthermore, by letting the number L of loci tend to infinity, a

continuous model, where $[0, 1]$ represents a whole chromosome (as in GRIFFITHS and MARJORAM (1997)), can be accommodated into our framework.

Correlations in coalescence times

The marginal process

Every marginal process (marginal with respect to one fixed locus under consideration) of our ancestral recombination graph is a Ξ -coalescent (see SCHWEINSBERG (2000a) for notation and details) with

$$\Xi = \delta_0 + c \frac{\psi^2}{4} \delta_{\left(\frac{\psi}{4}, \frac{\psi}{4}, \frac{\psi}{4}, \frac{\psi}{4}, 0, 0, \dots\right)}.$$

For $r = 0$, all marginals are identical (realization wise), in particular times to the most recent common ancestor for different loci have correlation 1. However, in contrast to the classical setting, for $r \rightarrow \infty$ one expects that the loci will not completely decorrelate, but instead keep positive correlations, as pointed out to us by J.E. Taylor (personal communication). In particular, one will not obtain the product distribution. This observation is a potential starting point for designing tests for the presence of large reproduction events, by comparing correlations for loci at large distance (hence with high recombination rate) under a Kingman- and a Ξ -coalescent based ARG.

Correlation in coalescence times at two loci

Correlations in coalescence times between two loci have been considered in the context of quantifying association between loci (MCVEAN, 2002). ELDON and WAKELEY (2008) consider correlations in coalescence times for a haploid population model admitting large offspring numbers, in which the ancestral process only admits asynchronous multiple mergers of ancestral lineages. To illustrate the effects of the reproduction parameters on the coalescence times, we also consider the probability that coalescence occurs at the same time at the two loci, as well as the expected time until coalescence.

The calculations to obtain the correlations for a sample of size two at two loci (following the approach and notation of DURRETT (2002)) are shown in the Appendix, Section 1.5. As we are now considering the gene genealogy of unlabelled lineages, let us briefly state the sample space. Let a and b denote the types at loci a and b , respectively. The three sample states before coalescence at either locus has occurred can be denoted as $(ab)(ab)$, $(ab)(a)(b)$, and $(a)(a)(b)(b)$. By $(ab)(ab)$ we denote the state of two chromosomes each carrying ancestral material at both loci. By $(ab)(a)(b)$ we denote the state of one (ab) chromosome in addition to two chromosomes (a) and (b) carrying ancestral types at locus 1 and 2 only, resp. The notation $(a)(a)(b)(b)$ denotes the state of four

chromosomes each carrying ancestral types at only one locus. Let

$$h(i) := \mathbb{P}(\{T_a = T_b\} | i), \quad i \in \{0, 1, 2\}$$

denote the probability that coalescence at the two loci occurs at the same time, given that the process starts in state i , in which i refers to the number of double-marked chromosomes (2, 1, or 0). As we are working with the limiting model, all marked individuals are effectively single-marked. Under the usual (Kingman coalescent-based) ARG, $\lim_{r \rightarrow \infty} h(i) = 0$ as one would expect. Our model yields

$$\lim_{r \rightarrow \infty} h(i) = \frac{c\psi^4}{32 + 8c\psi^2 - c\psi^4}, \quad i \in \{0, 1, 2\}; \quad (31)$$

indicating that even unlinked loci remain correlated due to sweepstake-style reproduction. Figure 2 shows graphs of $h(i)$ as a function of ψ for different values of c and r . As expected, $h(i)$ increases with ψ , at a rate which increases with c .

Under the usual ARG, the expected time $\mathbb{E}_i[T_s]$ until coalescence at either loci, starting from state i is given by $\mathbb{E}_i[T_s] = (1 + h(i))/2$. The random variable T_s can be viewed as the minimum of the time until coalescence occurs at the two loci. As $r \rightarrow \infty$, the times T_1 and T_2 until coalescence at the two loci, resp., become independent and identically distributed exponentials (i.i.d.e.) with rate 1, whose minimum has expected value $1/2$. Under our model, the mean of T_s is *not* the minimum of two i.i.d.e. with rate $1 + c\psi^2/4$, another reflection of the correlation in gene genealogies induced by sweepstake-style reproduction. Indeed, our model gives

$$\lim_{r \rightarrow \infty} \mathbb{E}_i[T_s] = \frac{1}{2} \left(\frac{1}{1 + \chi c\psi^2/4} \right), \quad i \in \{0, 1, 2\}.$$

in which $\chi = 1 - \psi^2/8$.

Under our model, $\mathbb{E}_i[T_s]$ decreases with ψ , and the rate of decrease increases with c (Figure 3). The same pattern holds for the expected time $\mathbb{E}_i[T_l]$ until coalescence has occurred at both loci (Figure 4). As $r \rightarrow \infty$, $\mathbb{E}_i[T_l]$ associated with the usual ARG approaches the expected value $(3/2)$

of the maximum of two i.i.d.e. with rate 1. Under our model,

$$\lim_{r \rightarrow \infty} \mathbb{E}_i[T_l] = \frac{3}{2} \frac{1}{1 + \frac{c\psi^2}{4}} \frac{1}{1 + \frac{c\psi^2}{4} - \frac{c\psi^4}{32}} + \frac{c\psi^2(6 - \psi^2)}{(c\psi^2 + 4)(4 + c\psi^2 - c\psi^4/8)}$$

while the maximum of two i.i.d.e. with rate λ has expected value $3/(2\lambda)$.

The correlation $\text{cor}_i(T_1, T_2)$ between T_1 and T_2 when starting from one of the three possible sample states $i \in \{0, 1, 2\}$ (see Appendix) increases with ψ , and more so if c is large (Figure 5). One obtains the following limit relations between $h(i)$ and $\text{cor}_i(T_1, T_2)$ for $i \in \{0, 1, 2\}$:

$$\begin{aligned} \lim_{r \rightarrow \infty} \text{cor}_i(T_1, T_2) &= \lim_{r \rightarrow \infty} h(i), \quad (\text{see Eq. (31)}); \\ \lim_{r \rightarrow 0} \text{cor}_i(T_1, T_2) &= \lim_{r \rightarrow 0} h(i), \quad (\text{see Eq. (70)}); \\ \lim_{c \rightarrow \infty} \text{cor}_i(T_1, T_2) &= \lim_{c \rightarrow \infty} h(i), \quad (\text{see Eq. (69)}). \end{aligned}$$

Quantifying the association between alleles at different loci can give insight into the evolutionary history of populations. Let f_a and f_b denote the frequencies of alleles a at locus 1, and b at locus 2, and let f_{ab} denote the frequency of chromosome ab in the total population. The statistic $D_{ab} := f_{ab} - f_a f_b$ measures the deviation from independence, since if the two loci were evolving independently, $f_{ab} = f_a f_b$. A related quantity is the r^2 statistic, defined as

$$r^2 := \frac{D^2}{f_a(1 - f_a)f_b(1 - f_b)}$$

(HILL and ROBERTSON, 1968), assuming $f_a, f_b \notin \{0, 1\}$. In applications, one would like to compare observed values of r^2 calculated from data to the expected value $\mathbb{E}[r^2]$, obtained under an appropriate population model. Calculating the expected value of r^2 is not straightforward, since r^2 is a ratio of correlated random variables. The expected value of r^2 is, instead, approximated by the ratio $\mathfrak{D} = \mathbb{E}[D^2]/\mathbb{E}[f_a(1 - f_a)f_b(1 - f_b)]$ (OHTA and KIMURA, 1971).

A prediction \mathfrak{D} of linkage disequilibrium in the population can be framed in terms of correlations in coalescence times between two loci for a sample of size two, assuming a small mutation rate (McVEAN, 2002). The prediction rests on approximating the expected value $\mathbb{E}[r^2]$ of the squared

correlation statistic r^2 (HILL and ROBERSON, 1968) of association between alleles at two loci by the ratio of expected values (OHTA and KIMURA, 1971). Following e.g. DURRETT (2002) one can obtain expressions for correlations in coalescence times between two loci for a sample of size two (see Appendix). Under our model, one obtains the limit results

$$\begin{aligned}\lim_{r \rightarrow \infty} \mathfrak{D} &= 0, \\ \lim_{c \rightarrow \infty} \mathfrak{D} &= \frac{\psi^3 - 16\psi^2 + 56\psi - 80}{\psi^3 - 10\psi^2 + 88\psi - 176}.\end{aligned}$$

When ψ is small but c large, one obtains

$$\mathfrak{D} = \frac{5 - 7\psi/2}{11 - 11\psi/2} + O(\psi^2).$$

Under the usual ARG, $\lim_{r \rightarrow 0} \mathfrak{D} = 5/11$. Thus, even in the presence of a *high* recombination rate, if large offspring number events are frequent enough, one may only see evidence of *low* recombination rate in data. Further, the prediction \mathfrak{D} can be substantially higher than Kingman-coalescent based predictions if c is large, and the recombination rate is not too small (Figure 6).

For particular examples of probability measures F from Equation (27) associated with the generator derived from our random offspring distribution model one can compute the quantities considered above in relation to fixed ψ . One such example distribution can be the Beta(ϑ, γ) distribution. One obtains for $i \in \{0, 1, 2\}$,

$$\lim_{r \rightarrow \infty} h(i) = \frac{4\gamma(1 + 2\vartheta + \gamma)}{8\gamma(1 + \gamma) + 10\gamma\vartheta + 7\vartheta(1 + \vartheta)}.$$

Define $\tilde{h}(i) := \lim_{r \rightarrow \infty} h(i)$. For $i \in \{0, 1, 2\}$ one obtains

$$\begin{aligned}\lim_{r \rightarrow \infty} \mathbb{E}_i[T_s] &= 4\tilde{h}(i) + \frac{4\gamma(1 + 2\vartheta + \gamma)}{8\gamma(1 + \gamma) + 10\gamma\vartheta + 7\vartheta(1 + \vartheta)}, \\ \lim_{r \rightarrow \infty} \mathbb{E}_i[T_l] &= \frac{3}{2} - \frac{1}{2}\tilde{h}(i) + \frac{3\gamma}{2(8\gamma(1 + \gamma) + 10\gamma\vartheta + 7\vartheta(1 + \vartheta))}.\end{aligned}\tag{32}$$

The form of the relation shown in (32) between $h(i)$ and $\mathbb{E}_i[T_s]$ and $\mathbb{E}_i[T_l]$ resembles the one obtained for the Kingman coalescent-based ARG, with the addition of a ‘correction’ term due to simultaneous multiple mergers.

Variance of pairwise differences

The expected variance of pairwise differences was employed by WAKELEY (1997) to estimate the recombination rate in low offspring number (Wright-Fisher) populations, under the usual ancestral recombination graph. Let the random variable K_{ij} denote the number of differences between sequences i and j , with $K_{ii} = 0$. The average number π of pairwise differences for n sequences is

$$\pi = \frac{2}{n(n-1)} \sum_{i < j} K_{ij}.$$

The (empirical) variance S_π^2 of pairwise differences is defined as

$$S_\pi^2 = \frac{2}{n(n-1)} \sum_{i < j} (K_{ij} - \pi)^2.$$

In the Appendix we derive the expected variance of pairwise differences $\mathbb{E}[S_\pi^2]$ under the ancestral recombination graph described by the generator G (14) derived from our large offspring number model. Under our model, $\mathbb{E}[S_\pi^2]$ is a function of the parameters c and ψ , in addition to being a function of r and θ (Figures 8 and 9). In Figure 8, $\mathbb{E}[S_\pi^2]$, when only two loci are considered, is graphed as a function of the recombination rate, and in Figure 9 as a function of sample size. Figures 8 and 9 show that $\mathbb{E}[S_\pi^2]$ is primarily influenced by the mutation rate (θ), when the values of c and ψ are fairly modest. However, $\mathbb{E}[S_\pi^2]$ can be quite low when both c and ψ are large, even when θ is also large (Figure 9). When c and ψ are both large, two sequences are more likely to coalesce before a mutation separates them.

The variance of pairwise differences alone will not suffice to yield estimates of r if both c and ψ are unknown. To jointly estimate the four parameters (c , ψ , r , θ) of our model one probably needs to employ computationally-heavy likelihood and importance sampling methods in the spirit of FEARNHEAD and DONNELLY (2001). However, given knowledge of c and ψ , one can, in principle, use the variance of pairwise differences to quickly obtain estimates of the recombination rate.

Correlations in ratios of coalescence times

The behaviour of the correlations in ratios of coalescence times for sample sizes larger than two is investigated using Monte Carlo simulations.

Let L_i denote the total length of branches ancestral to i sequences at one locus, let L denote the total length of the genealogy at the same locus, and define $R_i := L_i/L$. Thus, R_1 is the total length of external branches to the total size of the genealogy. The idea behind estimating

the expected value $\mathbb{E}[R_i]$ is as follows. Assuming the infinitely many sites mutation model, let S_i denote the total number of mutations in i copies, S the total number of segregating sites, and define $V_i := S_i/S$. The key idea behind deriving the coalescent was to separate the (neutral) mutation process from the genealogical process. The same principle also applies to predicting patterns of genetic variation using the coalescent: first one constructs the genealogy, and then superimposes mutations on the genealogy. The shape of the genealogy is thus a deciding factor in the genetic patterns one predicts. The relative lengths R_i of the different types of branches should therefore predict the relative number V_i of mutations of each class. This idea is exploited by ELDON (2011) to estimate coalescence parameters in the large offspring number models introduced by SCHWEINSBERG (2003) and ELDON and WAKELEY (2006). Namely, the claim is

$$\lim_{n \rightarrow \infty} \mathbb{E}[R_i] = \lim_{n \rightarrow \infty} \mathbb{E}[V_i] = f(\varpi, i) \quad (33)$$

where n denotes the sample size, ϖ denotes the coalescence (reproduction) parameters. Indeed, it follows from the results of BERESTYCKI *et al.* (2007, 2008), that ($1 < \alpha < 2$)

$$\lim_{n \rightarrow \infty} \mathbb{E}[R_i] = \lim_{n \rightarrow \infty} \mathbb{E}[V_i] = \frac{\Gamma(i+\alpha-2)(\alpha-1)(2-\alpha)}{\Gamma(\alpha)!}$$

when associated with the Beta($2 - \alpha, \alpha$) coalescent derived by SCHWEINSBERG (2003) from a population model in which the offspring law is stable with index α . A key feature of expression (33) is the absence of mutation rate in the function $f(\varpi, i)$; thus given large number of DNA sequences (possibly in the thousands), one hopes to be able to obtain estimates of the coalescence parameters ϖ without having to jointly estimate the mutation rate. In our model, there are four parameters to estimate, namely mutation and recombination rates, along with the coalescence parameters c and ψ . Even though full likelihood methods exist (BIRKNER and BLATH, 2008; BIRKNER *et al.*, 2011), applying them to large datasets consisting of thousands of sequences may represent a challenge.

Estimates of $\mathbb{E}[R_i]$ as functions of the sample size n , and the coalescence parameters c and ψ are shown in Table 4. In nearly all cases the estimates \bar{R}_i decreased as sample size increased; the exception was \bar{R}_1 when $(c, \psi) = (1000, 0.5)$ (Table 4). When both c and ψ are large enough, we observe a non-monotonic behaviour in \bar{R}_1 as sample size increases (results not shown). The non-monotonic behaviour may be related to the property of the marginal haploid process (the point-

mass part obtained as $c \rightarrow \infty$) of a single locus of not coming down from infinity (SCHWEINSBERG, 2000b), i.e. when one starts with an infinite number of lineages (sample size), the number of lineages stays infinite. For such processes that don't come down from infinity, the ratio R_1 should go to one, i.e. the gene genealogy should become completely star-shaped (see e.g. ELDON (2011)). As both c and ψ increase, one expects the deviation from Kingman-coalescent based predictions to increase. By way of example, for sample size 50 the vector $(\mathbb{E}[R_1], \dots, \mathbb{E}[R_4])$ is estimated to be approx. (0.24, 0.12, 0.08, 0.06) when associated with the Kingman coalescent ($c = 0$), while being approx. (0.58, 0.20, 0.09, 0.05) when $(c, \psi) = (1000, 0.5)$. In all cases the estimate \widehat{R}_i of the standard deviation of R_i decreases as sample size increases, indicating convergence.

The rationale behind comparing the statistics in Tables (5–6) is as follows. As sequencing technologies advance, and the genomic sequences of more organisms become available, a case in point being the recently published genomic sequence of Atlantic cod (STAR *et al.*, 2011), genomic scans of thousands of individuals will become more common. Given DNA sequence data for many loci, one could calculate correlations for counts and ratios of counts of mutations, and compare them to predictions based on different ancestral recombination graphs. Similarly for the single-locus statistics (Table 4), the idea is that the correlations of the coalescence time statistics (L_i and R_i) should reflect correlations of mutation counts (S_i). In particular, under the usual ARG one expects (see Tables 5–6)

$$\lim_{r \rightarrow \infty} \text{cor} \left(L_i^{(1)}, L_j^{(2)} \right) = \lim_{r \rightarrow \infty} \text{cor} \left(R_i^{(1)}, R_j^{(2)} \right) = 0,$$

where the superscript refers to locus number one and two, respectively, while under an ARG admitting simultaneous multiple mergers one expects

$$\begin{aligned} \lim_{r \rightarrow \infty} \text{cor} \left(L_i^{(1)}, L_j^{(2)} \right) &= f(i, j, \varpi) \\ \lim_{r \rightarrow \infty} \text{cor} \left(R_i^{(1)}, R_j^{(2)} \right) &= g(i, j, \varpi) \end{aligned}$$

where f and g are functions of the particular statistics indicated by i and j as well as the vector ϖ of coalescence (reproduction) parameters.

In general, the results reported in Tables 5–6 indicate that high values of *both* ψ and c are required for high correlations when recombination rate is high, when associated with our model. In

particular, the correlations between $R_i^{(1)}$ and $R_i^{(2)}$ (i.e. between corresponding R_i 's at different loci) can be quite high, even when recombination is high, when both c and ψ are large enough; another indicator of the genome-wide correlations induced by sweepstake-like reproduction.

A different question concerns the limit behaviour as sample size n increases. Fix the recombination rate and consider the limits

$$\lim_{n \rightarrow \infty} \text{cor} \left(R_i^{(1)}, R_j^{(2)} \right), \quad \lim_{n \rightarrow \infty} \text{cor} \left(V_i^{(1)}, V_j^{(2)} \right) \quad (34)$$

Under the usual ARG, one expects the limits in (34) to be only functions of the recombination rate (and i and j). If the ARG also admits simultaneous multiple mergers, one expects the limits in (34) also to be functions of ϖ . Considering unlinked loci, one would be interested in the limits

$$\lim_{r \rightarrow \infty} \lim_{n \rightarrow \infty} \text{cor} \left(R_i^{(1)}, R_j^{(2)} \right), \quad \lim_{r \rightarrow \infty} \lim_{n \rightarrow \infty} \text{cor} \left(V_i^{(1)}, V_j^{(2)} \right) \quad (35)$$

Resolving the limits (35) for different ARG's promises not only to yield insights into genome-wide correlations, but also to provide tools for inference; e.g. to distinguish between different population models.

The C program written to perform the simulations was checked by comparing correlation in coalescence times for sample size two at two loci to analytical results. The program is available upon request.

Comparison with ELDON and WAKELEY (2008)

ELDON and WAKELEY (2008) consider correlations in coalescence times, and the prediction \mathfrak{D} of linkage disequilibrium, under a modified Wright-Fisher sweepstake-style reproduction model, and observe correlations in coalescence times between loci despite high recombination rate. Our work differs from theirs in important ways. To begin with, we treat diploidy in detail, in which each offspring receives its two chromosomes from two distinct diploid parents. This leads to a separation of timescales of the ancestral process. We formally derive an ancestral recombination graph which admits simultaneous multiple mergers of ancestral lineages, which naturally arise in diploid models. Eldon and Wakeley observed correlations in coalescence times when considering only sample size two at each locus in a model that contains diploid individuals only implicitly, it is not a priori obvious that the correlations would still hold for large sample sizes. We confirm this using our

formally obtained ARG, that allows us also to investigate correlations in coalescence times, and in ratios of coalescence times, for sample sizes larger than two at each locus. In addition, one can apply our ARG to inference problems. Indeed, we show how the variance of pairwise differences can, in principle, be used to obtain estimates of the recombination rate. Finally, we obtain a large class of ARGs by randomizing the offspring distribution; thus one is not restricted to the simple case of fixed ψ .

Furthermore, since the estimate \mathfrak{D} of the expected value of r^2 can be expressed in terms of correlations in coalescence times, Eldon and Wakeley consider \mathfrak{D} under their modified Wright-Fisher model. However, \mathfrak{D} is based on approximating an expected value of a ratio of correlated random variables by the ratio of expected values of the corresponding random variables, and is also derived for a sample of size two at two loci. Thus, \mathfrak{D} may not be the ideal quantity to quantify association between loci for large sample sizes. A more natural way may be to investigate correlations in coalescence times for samples larger than two the way we do.

Discussion

Understanding the genome-wide effects of sweepstake-like reproduction on gene genealogies was our main aim. To this end, we derived ancestral recombination graphs for many loci arising from population models admitting large offspring numbers. High variance in individual reproductive success, or sweepstake-style reproduction, has been suggested to explain the low genetic diversity observed in many marine populations (HEDGECOCK *et al.*, 1982; HEDGECOCK, 1994; AVISE *et al.*, 1988; PALUMBI and WILSON, 1990; BECKENBACH, 1994; ÁRNASON, 2004). HEDGECOCK and PUDOVKIN (2011) review the sweepstake-style reproduction hypothesis, and conclude that it provides the correct framework in which to investigate many natural marine populations.

Multiple (DONNELLY and KURTZ, 1999; PITMAN, 1999; SAGITOV, 1999) and simultaneous (SCHWEINSBERG, 2000a; MÖHLE and SAGITOV, 2001) multiple merger coalescent models arise from population models incorporating sweepstakes reproduction by admitting large offspring numbers (SAGITOV, 2003; ELTON and WAKELEY, 2006; SARGSYAN and WAKELEY, 2008). While multiple merger coalescent processes describing the ancestral relations of alleles at a single locus have received the most attention from mathematicians, ancestral processes for multiple linked loci have hitherto remained unexplored. We derive an ancestral recombination graph for many loci from a diploid biparental population model, in which one pair of diploid individuals (parents) contribute

offspring to the population at each timestep. Thus, each offspring necessarily receives her chromosomes from distinct individuals, as diploid individuals tend to do. Incorporating diploidy into our model the way we do leads to a separation of timescales problem. Our limiting object is essentially a ‘haploid’ process, in which chromosomes either coalesce or recombine. By extending a result of MÖHLE (1998), we show that diploidy, a fundamental characteristic of many natural populations, can thus be treated as a ‘black box’, since the limiting object does not depend on the location of chromosomes in individuals.

By adopting a Moran type model, in which only a single pair of individuals gives rise to offspring at each reproduction event, we chose mathematical tractability over more biologically realistic scenarios; in which, for example, many individuals contribute offspring at each timestep. It should be straightforward to extend our model in many ways, for example allowing random number of parents, or introducing population structure. Indeed, we do extend our model in one way, by taking a random offspring distribution. These extensions still leave open the question of distinguishing among different large offspring number models. Our work on ancestral recombination graphs incorporating information from many loci is a step in this direction.

Sweepstake-style reproduction induces correlation in coalescence times even between loci separated by high rate of recombination. The correlation follows from the multiple merger property of our ancestral recombination graph, since many chromosomes coalesce at the same time in a multiple merger event. The correlation remains a function of the coalescence parameters (c and ψ) of our population model. An immediate question is the effects on predictions of linkage disequilibrium (LD). The approximation \mathfrak{D} by MCVEAN (2002) predicts low LD when recombination rate is high. However, when the rate of large reproduction events is high ($c \rightarrow \infty$), \mathfrak{D} remains a function of the coalescence parameters. The dependence of \mathfrak{D} on coalescence parameters has implications for the use of LD in inference for populations exhibiting sweepstake-style reproduction. Using simulations, DAVIES *et al.* (2007) found little effect of multiple mergers on the prediction r^2 of linkage disequilibrium, when comparing the exact Wright-Fisher model with recombination to the usual (continuous-time) ARG. However, by directly incorporating large offspring number events the way we do, we can show that large offspring number events do induce correlation in coalescence times, and hence influence predictions of linkage disequilibrium.

The genome-wide correlation in coalescence times (Tables 5–6) induced by sweepstake-style

reproduction offers hints about how to distinguish between large offspring number and ordinary Wright-Fisher reproduction. We are unaware of any published multi-loci methods derived to distinguish among different population models. Full likelihood methods may be preferable to the simple moment-based methods we consider. However, likelihood-based inference tends to be computationally intensive, and more so for large samples. For large samples, one should be able to quickly obtain a good idea of the underlying processes by comparing correlations in ratios of mutation counts with predictions based on different population models.

In conclusion, ancestral recombination graphs admitting simultaneous multiple mergers of ancestral lineages are derived from a diploid population model of sweepstake-style reproduction, suggested to be common in many diverse marine populations. Our calculations show that sweepstake-style reproduction results in genome-wide correlation of gene genealogies, even for large sample sizes. Estimates of linkage disequilibrium and of recombination rates are confounded by the coalescence parameters of our population model. The genome-wide correlation in gene genealogies induced by sweepstake-style reproduction implies that examining correlations between loci should provide means of distinguishing between ordinary Wright-Fisher and sweepstake-style reproduction.

We gratefully acknowledge the comments of two anonymous referees which helped to improve the presentation; one referee also spotted an error in our original proof of Theorem 1.3.

B.E. was supported in part by EPSRC grant EP/G052026/1, and by a Junior Research Fellowship at Lady Margaret Hall, Oxford. J.B. and B.E. were supported in part by DFG grant BL 1105/3-1. J.B. and B.E. would like to thank Institut für Mathematik, Johannes-Gutenberg-Universität Mainz, for hospitality. M.B. was in part supported by DFG grant BI 1058/2-1 and through ERC Advanced Grant 267356 VARIS. M.B. would like to thank Mathematisch Instituut, Universiteit Leiden, for hospitality.

References

- ÁRNASON, E., 2004 Mitochondrial cytochrome *b* variation in the high-fecundity Atlantic cod: trans-Atlantic clines and shallow gene genealogy. *Genetics* **166**: 1871–1885.
- AVISE, J. C., R. M. BALL, and J. ARNOLD, 1988 Current versus historical population sizes in vertebrate species with high gene flow: a comparison based on mitochondrial DNA lineages and inbreeding theory for neutral mutations. *Mol Biol Evol* **5**: 331–344.
- BECKENBACH, A. T., 1994 Mitochondrial haplotype frequencies in oysters: neutral alternatives

- to selection models. In B. Golding, editor, *Non-neutral Evolution*. Chapman & Hall, New York, 188–198.
- BERESTYCKI, J., N. BERESTYCKI, and J. SCHWEINSBERG, 2007 Beta-coalescents and continuous stable random trees. *Ann Probab* **35**: 1835–1887.
- BERESTYCKI, J., N. BERESTYCKI, and J. SCHWEINSBERG, 2008 Small-time behavior of beta coalescents. *Ann Inst H Poincaré Probab Statist* **44**: 214–238.
- BIRKNER, M., and J. BLATH, 2008 Computing likelihoods for coalescents with multiple collisions in the infinitely many sites model. *J Math Biol* **57**: 435–465.
- BIRKNER, M., and J. BLATH, 2009 Measure-valued diffusions, general coalescents and population genetic inference. In J. Blath, P. Mörters and M. Scheutzow, editors, *Trends in stochastic analysis*. Cambridge University Press, 329–363.
- BIRKNER, M., J. BLATH, M. MÖHLE, M. STEINRÜCKEN, and J. TAMS, 2009 A modified lookdown construction for the Xi-Fleming-Viot process with mutation and populations with recurrent bottlenecks. *ALEA Lat. Am. J. Probab. Math. Stat.* **6**: 25–61.
- BIRKNER, M., J. BLATH, and M. STEINRÜCKEN, 2011 Importance sampling for Lambda-coalescents in the infinitely many sites model. *Theor Popul Biol* **79**: 155–173.
- CANNINGS, C., 1974 The latent roots of certain Markov chains arising in genetics: A new approach, I. Haploid models. *Adv Appl Probab* **6**: 260–290.
- DAVIES, J. L., F. SIMANČÍK, R. LYNGSØ, T. MAILUND, and J. HEIN, 2007 On recombination-induced multiple and simultaneous coalescent events. *Genetics* **177**: 2151–2160.
- DONNELLY, P., and T. G. KURTZ, 1999 Particle representations for measure-valued population models. *Ann Probab* **27**: 166–205.
- DURRETT, R., 2002 *Probability models for DNA sequence evolution*. Springer, New York.
- ELDON, B., 2011 Estimation of parameters in large offspring number models and ratios of coalescence times. *Theor Popul Biol* **80**: 16–28.
- ELDON, B., and J. WAKELEY, 2006 Coalescent processes when the distribution of offspring number among individuals is highly skewed. *Genetics* **172**: 2621–2633.
- ELDON, B., and J. WAKELEY, 2008 Linkage disequilibrium under skewed offspring distribution among individuals in a population. *Genetics* **178**: 1517–1532.
- ETHERIDGE, A. M., R. C. GRIFFITHS, and J. E. TAYLOR, 2010 A coalescent dual process in

- a Moran model with genic selection, and the Lambda coalescent limit. *Theor Popul Biol* **78**: 77–92.
- FEARNHEAD, P., and P. DONNELLY, 2001 Estimating recombination rates from population genetic data. *Genetics* **159**: 1299–1318.
- GRIFFITHS, R. C., 1991 The two-locus ancestral graph. In I. V. Basawa and R. L. Taylor, editors, *Selected Proceedings of the Symposium on Applied Probability*. Institute of Mathematical Statistics, Hayward, CA, USA, 100–117.
- GRIFFITHS, R. C., and P. MARJORAM, 1997 An ancestral recombination graph. In P. Donnelly and S. Tavaré, editors, *Progress in Population Genetics and Human Evolution*, volume IMA Volumes in Mathematics and its Applications, 87. Springer, New York, 257–270.
- HARTL, D. L., and A. G. CLARK, 1989 *Principles of population genetics*. Sinauer, Sunderland, 2nd edition.
- HEDGECOCK, D., 1994 Does variance in reproductive success limit effective population sizes of marine organisms? In A. Beaumont, editor, *Genetics and evolution of Aquatic Organisms*. Chapman and Hall, London, 1222–1344.
- HEDGECOCK, D., and A. I. PUDOVKIN, 2011 Sweepstakes reproductive success in highly fecund marine fish and shellfish: a review and commentary. *Bull Marine Science* **87**: 971–1002.
- HEDGECOCK, D., M. TRACEY, and K. NELSON, 1982 Genetics. In L. G. Abele, editor, *The Biology of Crustacea*, volume 2. Academic Press, New York, 297–403.
- HERBOTS, H. M., 1997 The structured coalescent. In P. Donnelly and S. Tavaré, editors, *Progress of Population Genetics and Human Evolution*. Springer, 231–255.
- HILL, W. G., and A. ROBERSON, 1968 Linkage disequilibrium in finite populations. *Theor Appl Genetics* **38**: 226–231.
- HILL, W. G., and A. R. ROBERTSON, 1968 Linkage disequilibrium in finite populations. *Theor Appl Genet* **38**: 226–231.
- HUDSON, R. R., 1983a Properties of a neutral allele model with intragenic recombination. *Theor Popul Biol* **23**: 183–201.
- HUDSON, R. R., 1983b Testing the constant-rate neutral allele model with protein sequence data. *Evolution* **37**: 203–217.
- HUILLET, T., and MÖHLE, 2011 On the extended Moran model and its relation to coalescents

- with multiple collisions. *Theor Popul Biol* : doi:10.1016/j.tpb.2011.09.004.
- HUTCHINGS, J. A., T. D. BISHOP, and C. R. MCGREGOR-SHAW, 1999 Spawning behaviour of Atlantic cod, *Gadus morhua*: evidence of mate competition and mate choice in a broadcast spawning. *Can J Fish Aquat Sci* **56**: 97–104.
- KINGMAN, J. F. C., 1982a The coalescent. *Stoch Proc Appl* **13**: 235–248.
- KINGMAN, J. F. C., 1982b On the genealogy of large populations. *J App Probab* **19A**: 27–43.
- KRONE, S. M., and C. NEUHAUSER, 1997 Ancestral processes with selection. *Theor Popul Biol* **51**: 210–237.
- MCVEAN, G. A., 2002 A genealogical interpretation of linkage disequilibrium. *Genetics* **162**: 987–991.
- MÖHLE, M., 1998 A convergence theorem for markoff chains arising in population genetics and the coalescent with selfing. *Adv Appl Prob* **30**: 493–512.
- MÖHLE, M., and S. SAGITOV, 2001 A classification of coalescent processes for haploid exchangeable population models. *Ann Probab* **29**: 1547–1562.
- MÖHLE, M., and S. SAGITOV, 2003 Coalescent patterns in diploid exchangeable population models. *J Math Biol* **47**: 337–352.
- NEUHAUSER, C., and S. M. KRONE, 1997 The genealogy of samples in models with selection. *Genetics* **145**: 519–534.
- NORDEIDE, J. T., and I. FOLSTAD, 2000 Is cod lekking or a promiscuous group spawner? *Fish and Fisheries* **1**: 90–93.
- NOTOHARA, M., 1990 The coalescent and the genealogical process in geographically structured population. *J Math Biol* **29**: 59–75.
- OHTA, T., and M. KIMURA, 1971 Linkage disequilibrium between two segregating nucleotide sites under the steady flux of mutations in a finite population. *Genetics* **68**: 571–580.
- PALUMBI, S. R., and A. C. WILSON, 1990 Mitochondrial DNA diversity in the sea-urchins *Strongylocentrotus purpuratus* and *Strongylocentrotus droebachiensis*. *Evolution* **44**: 403–415.
- PITMAN, J., 1999 Coalescents with multiple collisions. *Ann Probab* **27**: 1870–1902.
- SAGITOV, S., 1999 The general coalescent with asynchronous mergers of ancestral lines. *J Appl Probab* **36**: 1116–1125.
- SAGITOV, S., 2003 Convergence to the coalescent with simultaneous mergers. *J Appl Probab*

40: 839–854.

SARGSYAN, O., and J. WAKELEY, 2008 A coalescent process with simultaneous multiple mergers for approximating the gene genealogies of many marine organisms. *Theor Pop Biol* **74**: 104–114.

SCHWEINSBERG, J., 2000a Coalescents with simultaneous multiple collisions. *Electron J Probab* **5**: 1–50.

SCHWEINSBERG, J., 2000b A necessary and sufficient condition for the λ -coalescent to come down from infinity. *Elect Comm Probab* **5**: 1–11.

SCHWEINSBERG, J., 2003 Coalescent processes obtained from supercritical Galton-Watson processes. *Stoch Proc Appl* **106**: 107–139.

STAR, B., A. J. NEDERBRAGT, S. JENTOFT, and U. G. ET AL, 2011 The genomic sequence of Atlantic cod reveals a unique immune system. *Nature* **477**: 207–210.

STEINRÜCKEN, M., M. BIRKNER, and J. BLATH, 2012 Analysis of DNA sequence variation within marine species using Beta-coalescents. *Theor Popul Biol* **to appear**.

TAJIMA, F., 1983 Evolutionary relationships of DNA sequences in finite populations. *Genetics* **105**: 437–460.

TAYLOR, J., and A. VÉBER, 2009 Coalescent processes in subdivided populations subject to recurrent mass extinctions. *Electron J Probab* **14**: 242–288.

TAYLOR, J. E., 2009 The genealogical consequences of fecundity variance polymorphism. *Genetics* **182**: 813–837.

WAKELEY, J., 1997 Using the variance of pairwise differences to estimate the recombination rate. *Genet. Res Camb* **69**: 45–48.

1 Appendix

1.1 Overview of transitions and their probabilities in the finite population model

1.1.1 Basic setup and notation

We will now classify all transitions and their probabilities of our population model relevant for the ancestral process under the scaling $\varepsilon_N = c/N^2$, in which N denotes the population size. Fix

a sample size n for this section. Usually we suppress the dependence on the sample size in the notation below. Recall the state space \mathcal{A}_n of our ancestral process (resp. $\mathcal{A}_n^{\text{sm}}$ for the ‘effective’ limiting model).

Let Π_N be the transition matrix of the Markov chain $\{\xi^{n,N}(m)\}_{m=0,1,\dots}$ on \mathcal{A}_n describing the ancestral states of an n -sample in a population of size N . Our aim is to decompose Π_N into

$$\Pi_N = A_N + \frac{1}{N^2} B_N + R_N \quad (36)$$

where the matrix A_N contains all transitions whose probability is $O(1)$ or $O(N^{-1})$ per generation, so that they will happen ‘instantaneously’ in the limit, and either are identity transitions, or projections from \mathcal{A}_n to $\mathcal{A}_n^{\text{sm}}$ by means of dispersing chromosomes paired in double-marked individuals. The matrix B_N contains all transition probabilities which are positive and finite after multiplication with N^2 and $N \rightarrow \infty$, that is, our ‘effective transitions’. The remainder matrix R_N carries only transition probabilities that are of order $O(N^{-3})$ or smaller, that will thus vanish after scaling.

Once we have established this decomposition, we can apply Lemma 1.7 below in a suitable way in order to identify the limit given in Definition 1.1 and establish the convergence result, i.e. Theorem 1.2.

In Tables 1 – 3 we will schematically deal with all possible transitions that can happen to a current sample over one timestep.

Analogous to the notation and convention of MÖHLE and SAGITOV (2003), we assume that in every configuration $\xi^{n,N}(m)$ from (2), the order of chromosomes in individuals \mathbb{I}_i for $i \in [b(m)]$ we have

$$\begin{aligned} \mathbb{I}_i(m) &= \left\{ C^{(2i-1)}(m), C^{(2i)}(m) \right\} \\ &\quad \text{if } 1 \leq i \leq \beta(m) - b(m); \\ \mathbb{I}_i(m) &= \left\{ C^{(\beta(m)-b(m)+i)}(m), \emptyset \right\} \\ &\quad \text{if } \beta(m) - b(m) + 1 \leq i \leq b(m). \end{aligned} \quad (37)$$

For ease of presentation, we denote by

\mathbb{I}' a single-marked individual carrying one active chromosome;

\mathbb{I}'' a double-marked individual carrying two active chromosomes;

$\tilde{\mathbb{I}}'$ a single-marked individual (parent) whose marked chromosome is not passed on in the sample during a given reproduction event;

$\hat{\mathbb{I}}''$ a double-marked individual (parent) where one marked chromosome is passed on and the other not during a given reproduction event.

The symbols (A) , (B) and (R) in the tables denote whether the corresponding transitions belong to A_N (A), to B_N (B) or the ‘remainder term’ (R) in (36) according to the decomposition mentioned above. After that, we compute all the important probabilities explicitly. The order of the probability of each transition is also noted in Tables 1–3.

1.1.2 Transition type 1: Small or large reproduction event, no offspring in the sample

If a reproduction event takes place, say at generation m , that does not affect our sample, this will not affect the state of our ancestral process at $m + 1$, and we have $\xi^{n,N}(m) = \xi^{n,N}(m + 1)$. Hence, we see an identity transformation. We now compute the probability that our sample is not affected. Given current state $\xi \in \mathcal{A}_n$ with b individuals and β chromosomes (hence $\beta - b$ double-marked and $2b - \beta$ single-marked individuals), the probability that no child is in the sample is

$$(1 - \varepsilon_N) \frac{N - b}{N} + \varepsilon_N \frac{\binom{N-b}{\lfloor \psi N \rfloor}}{\binom{N}{\lfloor \psi N \rfloor}} = 1 - O(N^{-1}).$$

1.1.3 Transition type 2: Small reproduction event, offspring in sample, at most one parent in the sample, no recombination

Here, we only need to distinguish whether the offspring is single or double marked, and whether there is a parent in the sample. For example, it is immediate to see that the probability of a transition from a double-marked (\mathbb{I}'') offspring to two single-marked ($\{\mathbb{I}', \mathbb{I}'\}$) individuals is of order $O(N^{-1})$ when no parent is in the sample and no recombination happens. Table 1 lists all corresponding events. By way of example, the state labelled $\{\mathbb{I}', \mathbb{I}'\}$ denotes that two single-marked individuals, each carrying one active chromosome, is reached from the sample configuration. One such configuration is if the sample contains one offspring, but neither parent (\emptyset), and the offspring is carrying two active chromosomes (\mathbb{I}'').

Table 1: Transitions of type 2.

Offspring	Parent with marked chromosome(s) (\emptyset means no parent in sample)	
	\emptyset	\mathbb{I}'
\mathbb{I}''	$\{\mathbb{I}', \mathbb{I}'\}$ (A) (* $O(N^{-1})$)	$\{\mathbb{I}', \mathbb{I}'\}, \{\mathbb{I}'', \mathbb{I}'\}$ $O(N^{-2}), (B)$
\mathbb{I}'	$\{\mathbb{I}'\}$ (A) (** $O(N^{-1})$)	$\{\mathbb{I}'\}, \{\mathbb{I}'', \mathbb{I}'\}, \{\mathbb{I}', \mathbb{I}'\}, (B)$ († $O(N^{-2})$)
	$\tilde{\mathbb{I}}'$	$\hat{\mathbb{I}}''$
\mathbb{I}''	$O(N^{-2}), (B)$	(‡ $O(N^{-2}), (B)$)
\mathbb{I}'	$\{\mathbb{I}''\}, \{\mathbb{I}', \mathbb{I}'\}, (B)$ $O(N^{-2})$	$\{\mathbb{I}', \mathbb{I}''\}, \{\mathbb{I}'\}, (B)$ $O(N^{-2})$

1.1.4 Transition type 3: Small reproduction event, offspring in sample, both parents in the sample

If both parents and offspring are in the sample in a small event, this immediately gives a transition probability of order $O(N^{-3})$ or smaller (depending on the presence of recombination, hence will be irrelevant, and be part of R_N . We omit a detailed table listing the different single- and double marked individuals.

1.1.5 Transition type 4: Small reproduction event, offspring and at most one parent in sample, recombination occurs

Table 2 lists transitions due to recombination, and when neither parent is in the sample. The probability of the presence of both an offspring and at least one parent in a sample, when recombination occurs, is of order $O(N^{-3})$, and so will vanish in the limit.

Table 2: Transitions of type 4, neither parent in sample

Offspring	Parent
	\emptyset
\mathbb{I}''	$\{\mathbb{I}'', \mathbb{I}'\}, O(N^{-2}), (B)$ $\{\mathbb{I}'', \mathbb{I}''\}, O(N^{-3}), (R)$
\mathbb{I}'	$\mathbb{I}'', O(N^{-2}), (B)$

1.1.6 Transition type 5: Large reproduction event, offspring in sample, no parent in sample, no recombination

Table 3 lists all possible transitions when a large reproduction event occurs, no parent is in the sample, and recombination does not occur. The probabilities of the events listed in Table 4 are of order $O(N^{-2})$, and so will appear as effective transitions in the limit.

Table 3: Transitions of type 5.

Offspring	Parent
	\emptyset
$k_1 \mathbb{I}', k_2 \mathbb{I}''$	$\{\mathbb{I}'', \mathbb{I}''\}, O(N^{-2}), (B)$
	$\{\mathbb{I}'', \mathbb{I}'\}, O(N^{-2}), (B)$
	$\{\mathbb{I}', \mathbb{I}'\}, O(N^{-2}), (B)$
	$\mathbb{I}'', O(N^{-2}), (B)$
	$\mathbb{I}', O(N^{-2}), (B)$

1.1.7 Transition type 6: Large reproduction event, offspring in sample, recombination occurs and / or at least one parent in sample

The probability that a large reproduction event takes place, at least one child and at least one parent are in the sample is $O(N^{-3})$. In addition, the probability that a large reproduction event takes place, at least one child is in the sample and also a recombination event happens in the sample is $O(N^{-3})$. Hence all such events are negligible.

1.2 The convergence result

1.2.1 The limit of the projection matrix A_N

Some care is needed in order to make sure A_N converges in the right sense to the desired projection matrix. The only relevant transitions of order $O(1)$ or $O(N^{-1})$ are transitions of type 1 and 2. The only one which is not an identity transition is the first dispersion event of Table 1. For $\xi \in \mathcal{A}_n$ with $b < \beta$ (i.e. at least one marked individual is double-marked), that is

$$\xi \mapsto \text{disp}_i(\xi).$$

This event will become part of A_N , and has probability

$$A_N(\xi, \text{disp}_i(\xi)) = (1 - \varepsilon_N) \frac{1}{N} \frac{\binom{N-b-1}{2}}{\binom{N}{2}} (1 - r_N)^2, \quad 1 \leq i \leq \beta - b \quad (38)$$

(this is the probability of the event (*) listed in row 1, column 1 of Table 1, note that the event (**) listed in row 2, column 1 there leads to an identity transition). Otherwise, we have

$$A_N(\xi, \xi) = 1 - (1 - \varepsilon_N) \frac{\beta - b}{N} \frac{\binom{N-b-1}{2}}{\binom{N}{2}} (1 - r_N)^2$$

Of course, A_N has to leave elements of the subspace $\mathcal{A}_n^{\text{sm}}$ invariant, hence we set, for ξ with $b = \beta$,

$$A_N(\xi, \xi') := \mathbf{1}_{\{\xi = \xi'\}}.$$

Proposition 1.4. *With the above settings, A_N is a stochastic matrix for each N and*

$$\lim_{C \rightarrow \infty} \lim_{N \rightarrow \infty} \sup_{r \geq CN} \|A_N^r - P\| = 0 \quad (39)$$

for all $C > 0$ large enough, where P is the canonical projection from \mathcal{A}_n to $\mathcal{A}_n^{\text{sm}}$, i.e.

$$P(\xi, \xi') = \mathbf{1}_{\{\xi' = \text{cd}(\xi)\}}.$$

Proof of Proposition 1.4 The Markov chain with transition matrix A_N can only change state by dispersing the chromosomes paired in a double-marked individual. We see from (38) that

$$A_N(\xi, \text{disp}_i(\xi)) \geq \frac{K(n, r, c)}{N}$$

for some suitable constant $K(n, r, c)$, uniformly in b and $i \leq \beta - b$ and N (for all N large enough). Hence, starting from ξ with $\beta - b$ double-marked individuals, the number of A_N -steps required until complete dispersion has occurred is dominated by the sum of $\beta - b$ independent geometric random variables $\gamma_1^{(N)} + \dots + \gamma_{\beta-b}^{(N)}$, with success probability $K(n, r, c)/N$. By Markov's inequality,

$$\sup_{N \in \mathbb{N}} \mathbb{P} \left\{ \gamma_1^{(N)} + \dots + \gamma_{\beta-b}^{(N)} \geq CN \right\} \leq \frac{1}{CN} \mathbb{E}[\gamma_1^{(N)} + \dots + \gamma_{\beta-b}^{(N)}] = \frac{N(\beta - b)}{C \cdot N \cdot K(n, r, c)} \rightarrow 0 \quad \text{as } C \rightarrow \infty.$$

The proof can now be completed with a coupling argument, noting that two Markov chains run according to A_N resp. P , started in $\xi \in \mathcal{A}_n$ get both stuck in $\text{cd}(\xi)$, and this happens after at most CN steps with high probability (for C large).

□

1.2.2 Proof of the convergence result

With the definition of A_N from the previous section, put

$$B_N^* := N^2(\Pi_N - A_N), \quad (40)$$

and let P be the canonical projection from \mathcal{A}_n to $\mathcal{A}_n^{\text{sm}}$ defined in Proposition 1.4. The following Lemma will identify G as the limit containing all the ‘effective’ transitions of B_N^* when projecting on the subspace $\mathcal{A}_n^{\text{sm}}$.

Lemma 1.5. *We have*

$$\widehat{B}_N := PB_N^*P \rightarrow G \quad \text{as } N \rightarrow \infty \quad (41)$$

with G from (14).

Remark 1.6. *We do believe that in fact the sequence of (formally larger) matrices B_N^* on \mathcal{A}_n converges as well, but the statement about \widehat{B}_N is sufficient for our purposes below (see (48) in Lemma 1.7) and simpler to prove since it allows to restrict to the ‘completely dispersed’ configurations in $\mathcal{A}_n^{\text{sm}}$.*

Proof of Lemma 1.5. We inspect the types of events listed in Tables 1-3 that are marked with (B). Events that are marked with (R) have probability of order at most $O(N^{-3})$, hence their total contribution to any entry of \widehat{B}_N is at most $O(N^{-1})$ (since we are following a finite sample, there are only finitely many possible one-step events altogether). It suffices to consider $\widehat{B}_N(\xi, \text{cd}(\eta))$ for $\xi = \{C^{(1)}, \dots, C^{(\beta)}; \beta\} \in \mathcal{A}_n^{\text{sm}}, \eta \in \mathcal{A}_n$ (because P projects to $\mathcal{A}_n^{\text{sm}}$).

Regarding $\xi' = \text{pairmerge}_{j_1, j_2}(\xi)$: This transition can happen in a small reproduction event (these events are listed at (†) in Table 1 in row 2, column 2, note that events listed at (‡) in Table 1 lead to a trivial transition once P is applied) or in a large reproduction event as in Table 3 if the grouping is suitable. Up to four parental chromosomes are involved in any reproduction event.

Hence, a large reproduction event can lead to a given pair merger in the sample if up to 5 individuals in the sample are children. Thus

$$\begin{aligned} \widehat{B}_N(\xi, \xi') = & N^2(1 - \varepsilon_N)(1 - r_N)2 \times \frac{1}{N} \frac{1 \cdot (N - b)}{\binom{N-1}{2}} \frac{1}{2} \frac{1}{2} \\ & + N^2 \varepsilon_N \sum_{c=2}^5 (1 - r_N)^c \binom{\beta - 2}{c - 2} \frac{\binom{N - \beta}{\lfloor N\psi \rfloor - c}}{\binom{N}{\lfloor N\psi \rfloor}} (4)_{c-1} \left(\frac{1}{4}\right)^c + O(N^{-1}) \end{aligned} \quad (42)$$

(For the first term on the right note that either j_1 or j_2 can be the child, the two factors of $\frac{1}{2}$ come from the requirement that the chromosome in the child we are following is the one from the parent in the sample and is also the one we are following in the parent. For the second term on the right note that once we decide on c children in the sample ($\binom{\beta-2}{c-2}$ choices because j_1 and j_2 are already chosen), there are $(4)_{c-1}$ ways to assign them to the 4 parental chromosomes. For comparison with (15) and the first line in (14) observe

$$\frac{\binom{N - \beta}{\lfloor N\psi \rfloor - c}}{\binom{N}{\lfloor N\psi \rfloor}} = \frac{(N - \beta)! \lfloor N\psi \rfloor! (N - \lfloor N\psi \rfloor)!}{(\lfloor N\psi \rfloor - c)! (N - \beta - \lfloor N\psi \rfloor + c)! N!} \sim \frac{(N\psi)^c (N(1 - \psi))^{\beta - c}}{N^\beta} = \psi^c (1 - \psi)^{\beta - c}.$$

Regarding $\xi' = \text{recomb}_{j,\ell}(\xi)$ (assuming that α is such that $C^{(j)}$ can be non-trivially cut into two by a recombination event between loci $\ell - 1$ and ℓ): This transition can happen in a small reproduction event as listed at (***) in Table 2 or in another event that has probability $O(N^{-3})$. Hence

$$\widehat{B}_N(\xi, \xi') = N^2(1 - \varepsilon_N) \times \frac{1}{N} \frac{\binom{N-b}{2} r^{(\ell)}}{\binom{N-1}{2}} + O(N^{-1}) = r^{(\ell)} + O(N^{-1}). \quad (43)$$

Regarding $\xi' = \text{groupmerge}_{J_1, J_2, J_3, J_4}(\xi)$: This can only occur through a large reproduction event as listed in Subsection 3. Write $k_i := |J_i|$, we assume $k_1 \geq \dots \geq k_a \geq 2$ for some $a \in [4]$, $k_{a+1} = \dots = k_4 = 0$ (if $a = 1$, $k_1 \geq 3$), $s := \beta - (k_1 + \dots + k_a)$ is the number of singletons (non-participating chromosomes) in the merger. Note that by the structure of the diploid model, with a groups merging there can be up to $k_1 + \dots + k_a + (4 - a)^+$ children in the sample (put

differently: up to $(4 - a)^+$ ‘non merging children’). Then

$$\begin{aligned} \widehat{B}_N(\xi, \xi') &= N^2 \varepsilon_N \sum_{c'=0}^{(4-a)^+} \binom{\beta - k_1 - \dots - k_a}{c'} (1 - r_N)^{k_1 + \dots + k_a + c'} \\ &\quad \times \frac{\binom{N - \beta}{\lfloor N\psi \rfloor - (k_1 + \dots + k_a + c')}}{\binom{N}{\lfloor N\psi \rfloor}} (4)_{a+c'} \left(\frac{1}{4}\right)^{k_1 + \dots + k_a + c'} \\ &\quad + O(N^{-1}). \end{aligned}$$

It remains to check that the diagonal terms behave correctly, i.e. that as $N \rightarrow \infty$,

$$\widehat{B}_N(\xi, \xi) \rightarrow G(\xi, \xi) = - \sum_{\xi' \neq \xi, \xi' \in \mathcal{A}_n^{\text{sm}}} G(\xi, \xi'). \quad (44)$$

Because Π_N and A_N are both stochastic matrices (as is P), we have

$$\widehat{B}_N(\xi, \xi) = - \sum_{\xi' \neq \xi, \xi' \in \mathcal{A}_n^{\text{sm}}} \widehat{B}_N(\xi, \xi') \quad (45)$$

for each N . By inspection and the discussion above, all terms in Π_N with decay rate $1/N$ are accounted for in A_N , and all non-diagonal terms in $\Pi_N - A_N$ with decay rate $1/N^2$ appear after multiplication with N^2 in \widehat{B}_N with their correct limits, namely the corresponding terms in G , while terms with a faster decay rate disappear in the limit. Hence (45) implies (44). \square

1.3 Markov chains with two time-scales — a variation on a lemma of Möhle

Conceptually, our convergence result rests on a separation of time-scales phenomenon. It can be established with the help of a variant of a well-know result, see Lemma 1 from MÖHLE (1998).

Let E be a finite set. We equip matrices $A = (A(x, y))_{x, y \in E}$ on E with the matrix norm $\|A\| := \max_{x \in E} \sum_{y \in E} |A(x, y)|$. Note that then $\|AB\| \leq \|A\| \|B\|$ and $\|A\| = 1$ if A is a stochastic matrix.

Lemma 1.7. *Assume that for $N \in \mathbb{N}$, A_N is a stochastic matrix on E such that*

$$\lim_{C \rightarrow \infty} \lim_{N \rightarrow \infty} \sup_{r \geq CN} \|A_N^r - P\| = 0 \quad (46)$$

for some matrix P . Then we have for any $0 < c, K, t < \infty$

$$\lim_{N \rightarrow \infty} \sup_{\|B\| \leq K} \|(A_N + cN^{-2} B)^{\lceil tN^2 \rceil} - (P + cN^{-2} B)^{\lceil tN^2 \rceil}\| = 0. \quad (47)$$

Furthermore, if $(B_N)_{N \in \mathbb{N}}$ is a sequence of matrices on E such that

$$G := \lim_{N \rightarrow \infty} PB_N P \quad \text{exists,} \quad (48)$$

then

$$\lim_{N \rightarrow \infty} (A_N + cN^{-2} B_N)^{\lceil tN^2 \rceil} = Pe^{ctG} \quad \text{for all } t > 0. \quad (49)$$

Remark 1.8. Instead of time scales N and N^2 one can allow more generally any $a_N, b_N \rightarrow \infty$ with $b_N/a_N \rightarrow \infty$, with only notational modifications in the proof.

Proof of Lemma 1.7. We begin with (47). W.l.o.g. assume $K = 1$, otherwise replace B by B/K and c by cK . Fix $c, t > 0$ and a matrix B with $\|B\| \leq 1$, abbreviate $m := \lceil tN^2 \rceil$. Let $\varepsilon > 0$, choose $C_0 < \infty$ and $N_0 \in \mathbb{N}$ such that

$$\|A_N^r - P\| \leq \varepsilon \quad \text{for } N \geq N_0, r \geq C_0 N \quad (50)$$

(as guaranteed by (46)). Note that

$$\begin{aligned} & \|(A_N + cN^{-2} B)^m - (P + cN^{-2} B)^m\| \\ & \leq \|A_N^m - P\| + \sum_{k=1}^m \left(\frac{c}{N^2}\right)^k \sum_{\substack{m_1, \dots, m_{k+1} \in \mathbb{N}_0 \\ m_1 + \dots + m_{k+1} = m-k}} \left\| A_N^{m_1} \prod_{j=2}^{k+1} (BA_N^{m_j}) - P^{m_1} \prod_{j=2}^{k+1} (BP^{m_j}) \right\|. \end{aligned}$$

Mimicking the proof in MÖHLE (1998), we split the second summand into (the ellipses refer to the term inside the large norm brackets on the right of the last line of the previous formula)

$$S_1 := \sum_{k=1}^m \left(\frac{c}{N^2}\right)^k \sum_{\substack{m_1, \dots, m_{k+1} \geq C_0 N \\ m_1 + \dots + m_{k+1} = m-k}} \dots \quad \text{and} \quad S_2 := \sum_{k=1}^m \left(\frac{c}{N^2}\right)^k \sum_{\substack{m_1, \dots, m_{k+1} \in \mathbb{N}_0 \\ m_1 + \dots + m_{k+1} = m-k \\ \exists j: m_j < C_0 N}} \dots$$

As in MÖHLE (1998), p. 509 we have $S_1 \leq 2e^t(t+1)\varepsilon$ for all N large enough, our estimate for S_2 is a small variation of the corresponding estimate in MÖHLE (1998): Note that each of the matrix norms appearing in the big sum in S_2 is at most 2, hence

$$\begin{aligned}
S_2 &\leq 2 \sum_{k=1}^m \left(\frac{c}{N^2}\right)^k \# \left\{ (m_1, \dots, m_{k+1}) \in \mathbb{N}_0^k : \begin{array}{l} m_1 + \dots + m_{k+1} = m - k, \\ \exists j : m_j < C_0 N \end{array} \right\} \\
&\leq 2 \sum_{k=1}^m \left(\frac{c}{N^2}\right)^k (k+1) \sum_{m_1=0}^{C_0 N \wedge (m-k)} \binom{m - m_1 - 1}{k-1} \\
&\leq 2 \sum_{k=1}^m \left(\frac{c}{N^2}\right)^k (k+1) C_0 N \binom{m-1}{k-1} = 2C_0 N \frac{c}{N^2} \sum_{k=0}^{m-1} \left(\frac{c}{N^2}\right)^k (k+2) \binom{m-1}{k} \\
&\leq C' \frac{1}{N}.
\end{aligned}$$

(We use in the last estimate that for $|x| < 1$, $n \in \mathbb{N}$, $\sum_{n=0}^{\infty} \binom{n}{k} x^k = (1+x)^n$ and $\sum_{n=0}^{\infty} k \binom{n}{k} x^k = nx(1+x)^{n-1}$.)

The derivation of (49) from (47) is literally the same as in MÖHLE (1998), p. 509-511 (read $c_N = c/N^2$ there). \square

1.4 The convergence result with general random Ψ_N

In this section we briefly indicate how the proof of Theorem 1.2 can be modified to yield Theorem 1.3. In each reproduction event, a random number Ψ_N of individuals die and are replaced by the same number of offspring, and recall Assumptions (20), (22) and (24). By “short” time-scale we refer to the scaling a_N given by

$$a_N = \frac{N}{\mathbb{E}[\Psi_N]}$$

and by “long” time-scale the scaling b_N given by

$$b_N = \frac{1}{c_N} = \frac{N(N-1)}{\mathbb{E}[\Psi_N(\Psi_N+3)]}.$$

Assumption (20) yields $b_N \rightarrow \infty$ as $N \rightarrow \infty$, and $b_N/a_N \rightarrow \infty$ by Assumption (21). To check (23), i.e. that indeed $a_N \rightarrow \infty$, observe that Ψ_N/N is a positive random variable, bounded by 1. Condition (20) is equivalent to $\mathbb{E}[(\Psi_N/N)^2] \rightarrow 0$, which implies $\Psi_N/N \rightarrow 0$ in probability and $\mathbb{E}[\Psi_N/N] \rightarrow 0$, hence (23).

For use below, we recall implications of (22) provided that (20) holds (cf SAGITOV (1999)):

$$\text{For all } j \geq 3 : \frac{1}{c_N} \mathbb{E} \left[\left(\frac{\Psi_N}{N} \right)^j \right] \xrightarrow{N \rightarrow \infty} \int_{[0,1]} x^{j-2} F(dx). \quad (51)$$

Indeed, integration by parts yields

$$\begin{aligned} \frac{1}{c_N} \mathbb{E} \left[\left(\frac{\Psi_N}{N} \right)^j \right] &= \frac{1}{c_N} \int_{(0,1]} j x^{j-1} \mathbb{P} \left(\frac{\Psi_N}{N} > x \right) dx \\ &\xrightarrow{N \rightarrow \infty} \int_{(0,1]} j x^{j-1} \int_{(x,1]} y^{-2} F(dy) dx = \int_{(0,1]} \left(\int_{(0,1]} 1_{\{x \leq y\}} j x^{j-1} dx \right) y^{-2} F(dy) \\ &= \int_{(0,1]} y^{j-2} F(dy). \end{aligned} \quad (52)$$

Furthermore for the case $j = 2$ one obtains

$$\limsup_{N \rightarrow \infty} \frac{1}{c_N} \mathbb{E} \left[\left(\frac{\Psi_N}{N} \right)^2 \right] = \limsup_{N \rightarrow \infty} \frac{\mathbb{E} [\Psi_N^2]}{\mathbb{E} [\Psi_N (\Psi_N + 3)]} \leq 1 < \infty. \quad (53)$$

Let $\tilde{\Psi}_N$ have the following reweighted distribution (relative to Ψ_N):

$$\mathbb{P}(\tilde{\Psi}_N = k) = \frac{k(k+3)}{\mathbb{E}[\Psi_N(\Psi_N+3)]} \mathbb{P}(\Psi_N = k), \quad k = 1, \dots, N-2, \quad (54)$$

then

$$\frac{\tilde{\Psi}_N}{N} \xrightarrow{d} F \quad \text{as } N \rightarrow \infty. \quad (55)$$

Indeed, for any $\ell \in \mathbb{N}$

$$\begin{aligned} \mathbb{E} \left[\left(\frac{\tilde{\Psi}_N}{N} \right)^\ell \right] &= \frac{N(N-1)}{\mathbb{E}[\Psi_N(\Psi_N+3)]} \mathbb{E} \left[\left(\frac{\Psi_N}{N} \right)^{\ell+1} \frac{\Psi_N+3}{N-1} \right] \\ &= \frac{1}{c_N} \mathbb{E} \left[\left(\frac{\Psi_N}{N} \right)^{\ell+2} \right] \frac{N}{N-1} + \frac{3}{(N-1)c_N} \mathbb{E} \left[\left(\frac{\Psi_N}{N} \right)^{\ell+1} \right] \xrightarrow{N \rightarrow \infty} \int_{(0,1]} y^\ell F(dy) \end{aligned} \quad (56)$$

by (52) and (53), so (55) follows because the moments characterise a probability law on $[0, 1]$. One can check (along the lines of SAGITOV (1999)) that under Assumption (20), both (52) and (55) are

in fact equivalent to (22).

The proof of Theorem 1.3 is now a relatively straightforward adaptation of the proof of Theorem 1.2 discussed in Sections 1.1 and 1.2 above. Scaling by N is throughout replaced by scaling with $a_N = N/\mathbb{E}[\Psi_N]$ and scaling by N^2 becomes scaling with $b_N = N(N-1)/\mathbb{E}[\Psi_N(\Psi_N+3)]$:

- (i) When currently following $b \geq 1$ individuals, the probability that none of them is an offspring in the previous reproduction event (and hence the sample configuration remains unchanged) is

$$\mathbb{E} \left[\frac{\binom{N-b}{\Psi_N}}{\binom{N}{\Psi_N}} \right] = \mathbb{E} \left[\prod_{j=0}^{\Psi_N-1} \frac{N-b-j}{N-j} \right] = \mathbb{E} \left[\prod_{j=0}^{\Psi_N-1} \left(1 - \frac{b}{N-j} \right) \right] = 1 - O \left(b \frac{\mathbb{E}[\Psi_N]}{N} \right) = 1 - O(a_N^{-1}).$$

This is analogous to transitions discussed in Section 1.1.2 and happens “all the time” (leading to the projecting transitions part in the limit).

- (ii) When currently following $b \geq 1$ individuals, say the i -th of which is double-marked, the probability that the i -th individual is the only offspring in the sample, and the sample also does not contain a parent, is (we write $(x)_k = x(x-1)\cdots(x-k+1)$ for the k -th falling factorial)

$$\mathbb{E} \left[\frac{\Psi_N(N-\Psi_N-2)_{b-1}}{(N)_b} \right] \sim \mathbb{E} \left[\frac{\Psi_N}{N} \left(1 - \frac{\Psi_N}{N} \right)^{b-1} \right] = a_N^{-1}(1 + o(1)).$$

The projection matrix A_N now becomes

$$A_N(\xi, \text{disp}_i(\xi)) = \mathbb{E} \left[\frac{\Psi_N(N-\Psi_N-2)_{b-1}}{(N)_b} \right] (1 - r_N)^2, \quad 1 \leq i \leq \beta - b \quad (57)$$

and $A_N(\xi, \xi) = 1 - (\beta - b)\mathbb{E} \left[\frac{\Psi_N(N-\Psi_N-2)_{b-1}}{(N)_b} \right] (1 - r_N)^2$; the analogue of Proposition 1.4 is then

$$\lim_{C \rightarrow \infty} \lim_{N \rightarrow \infty} \sup_{r \geq Ca_N} \|A_N^r - P\| = 0. \quad (58)$$

- (iii) From now on we can work on the “projected” space $\mathcal{A}_n^{\text{sm}}$. The distinction between small and large reproduction events is irrelevant in the general case. Hence, it is more suitable to distinguish whether a parent and an offspring are in the sample or whether several offspring (but no parent) is in the sample. In analogy with (40) and (41), we split Π_N into “fast” and

“slow” parts and define

$$B_N^* := b_N(\Pi_N - A_N), \quad \widehat{B}_N := PB_N^*P. \quad (59)$$

It then remains to check that

$$\widehat{B}_N \rightarrow G \quad \text{with } G \text{ defined in (26),} \quad (60)$$

whence Theorem 1.3 follows from Lemma 1.7 together with Remark 1.8.

We now verify (60):

(iv) Recombination events: These give the correct limit, see the discussion below (24).

(v) “Large:” The probability that exactly $k \geq 2$ individuals among b (excluding the parents) is, using (54),

$$\mathbb{E} \left[\frac{(\Psi_N)_k (N - \Psi_N - 2)_{b-k}}{(N)_b} \right] = \mathbb{E} [\Psi_N (\Psi_N + 3)] \mathbb{E} \left[\frac{(\widetilde{\Psi}_N)_k (N - 2 - \widetilde{\Psi}_N)_{b-k}}{\widetilde{\Psi}_N (\widetilde{\Psi}_N + 3) (N)_b} \right], \quad (61)$$

thus $1/c_N$ times this probability is

$$\begin{aligned} N(N-1) \mathbb{E} \left[\frac{(\widetilde{\Psi}_N)_k (N - 2 - \widetilde{\Psi}_N)_{b-k}}{\widetilde{\Psi}_N (\widetilde{\Psi}_N + 3) (N)_b} \right] &= \frac{1}{(N-2)_{b-2}} \mathbb{E} \left[(\widetilde{\Psi}_N - 2)_{k-2} (N - 2 - \widetilde{\Psi}_N)_{b-k} \right] + O\left(\frac{1}{N}\right) \\ &\xrightarrow{N \rightarrow \infty} \int_{(0,1]} y^{k-2} (1-y)^{b-k} F(dy) \end{aligned} \quad (62)$$

by (55). Furthermore, the probability that at least 2 offspring *and* at least one parent are in the sample is at most

$$b \binom{b-1}{2} \mathbb{E} \left[\frac{2(\Psi_N)_2}{(N)_3} \right] = O(c_N/N) \quad (63)$$

hence such events become negligible in the limit.

(vi) “Small” (=a merger of a single pair, which can result either from one offspring and one parent in the sample, or from two offspring but no parent in the sample): Here, the weight of $F(\{0\})$ plays a role.

The probability that exactly two given single-marked individuals in a sample of size b are offspring (and none are parents) is

$$\mathbb{E} \left[\frac{(\Psi_N)_2 (N - 2 - \Psi_N)_{b-2}}{(N)_b} \right], \quad (64)$$

and the probability that among a pair of two given single-marked individuals, one is a parent, the other an offspring and no other element of the sample is affected by the reproduction event is

$$\mathbb{E} \left[\frac{2(2)_1 (\Psi_N)_1 (N - \Psi_N - 2)_{b-2}}{(N)_b} \right], \quad (65)$$

thus, $1/c_N$ times the probability that exactly one given pair (of single-marked individuals) is involved in a reproduction event is

$$\begin{aligned} \frac{1}{c_N} \mathbb{E} \left[\frac{\Psi_N (\Psi_N + 3) (N - \Psi_N - 2)_{b-2}}{(N)_b} \right] &= \mathbb{E} \left[\frac{(N - 2 - \tilde{\Psi}_N)_{b-2}}{(N - 2)_{b-2}} \right] \\ &\xrightarrow{N \rightarrow \infty} \int_{[0,1]} (1 - y)^{b-2} F(dy) = F(\{0\}) + \int_{(0,1]} (1 - y)^{b-2} F(dy) \end{aligned} \quad (66)$$

by (55).

- (vii) (Combinatorial connections between participation in reproduction events and merging of ancestral chromosomes) The rest of the argument in order to replace (15) by (27) is purely combinatorial; it is only concerned with possible groupings of the k single-marked offspring into up to four groups depending on which of the four parental chromosomes they descend from.

In both cases considered in (6) the probability that the chromosomes actually coalesce is $\frac{1}{4}$ because they must descend from the same chromosome in the same parent, or from the particular chromosome in the particular parent we are following, respectively.

1.5 Correlation in coalescence times

In this section we outline the calculations to obtain the correlation in coalescence times T_1 and T_2 of types at two loci (1 and 2). As our sample consists of two unlabelled chromosomes typed at two

loci, we will sometimes find it convenient to denote an unlabelled chromosome carrying ancestral segments at both loci with the symbol \vdash , while chromosomes carrying ancestral segments at only one locus with the symbols \vdash and \dashv . Loci at which types have coalesced will be denoted by \bullet , or $\bullet\vdash$. The states \mathfrak{S} of the unlabelled process for a sample of size two at two loci will also be numbered as follows:

\mathfrak{S}	in symbols
2	$(\vdash)(\vdash)$
1	$(\vdash)(\vdash)(\dashv)$
0	$(\vdash)(\vdash)(\dashv)(\dashv)$
-1	$(\dashv)(\dashv)$
-2	$(\vdash)(\vdash)$

in which states $\{0, 1, 2\}$ denote the three possible sample states, before coalescence at either loci has occurred. States $\{-1, -2\}$ will be needed when deriving the variance of pairwise differences.

Let $h(i) := \mathbb{P}(\{T_1 = T_2\}|i)$ denote the probability of the event $T_1 = T_2$, when B is in state i . Excluding large offspring numbers, one readily obtains ($h(i) = 0$ for $i \neq \{0, 1, 2\}$)

$$\begin{aligned}
 h(2) &= \frac{r+9}{2r^2+13r+9} \\
 h(1) &= \frac{3}{2r^2+13r+9} \\
 h(0) &= \frac{2}{2r^2+13r+9}
 \end{aligned} \tag{67}$$

For each $i \in \{0, 1, 2\}$, the expression for $h(i)$ is the same as the one for the correlation between T_1 and T_2 when in state i , excluding large offspring numbers. The expected value $w(i) = \mathbb{E}_i[T_s]$ of the time T_s until a coalescence event at either locus starting from state $i \in \{0, 1, 2\}$ is, again excluding

large offspring numbers,

$$\begin{aligned} w(2) &= \frac{r+9}{2(2r^2+13r+9)} + \frac{1}{2} = \frac{1}{2} (1 + h(2)) \\ w(1) &= \frac{3}{2(2r^2+13r+9)} + \frac{1}{2} = \frac{1}{2} (1 + h(1)), \\ w(0) &= \frac{1}{2r^2+13r+9} + \frac{1}{2} = \frac{1}{2} (1 + h(0)), \end{aligned}$$

obtained by solving the recursions

$$\begin{aligned} w(2) &= (1 + 2rw(1))/(1 + 2r) \\ w(2) &= (1 + 2rw(1))/(1 + 2r) \\ w(1) &= (1 + w(2) + rw(0))/(r + 3) \\ w(0) &= (1 + 4w(1))/6 \end{aligned}$$

Let $v(i) := \mathbb{E}_i[T_s^2]$ denote the expected value of T_s^2 when starting from state $i \in \{0, 1, 2\}$. One can follow DURRETT (2002) to obtain the recursions

$$v(i) = \frac{2}{q_i^2} + \frac{2}{q_i} \sum_{k \neq i} \frac{q_{ik}}{q_i} w(k) + \sum_{k \neq i} \frac{q_{ik}}{q_i} v(k) \quad (68)$$

in which $q_i = \sum_{k \neq i} q_{ik}$ is the sum of the transition rates out of state i . To obtain (68) let J denote the exponential waiting time until the first transition, and X_J the state of the process immediately after the first transition. The random variables J and X_J are independent. One can write

$$\begin{aligned} \mathbb{E} [T_s^2 | J, X_J] &= \mathbb{E} [(T_s - J + J)(T_s - J + J) | J, X_J] \\ &= \mathbb{E} [(T_s - J)^2 + 2J(T_s - J) + J^2 | J, X_J] \\ &= \mathbb{E} [(T_s - J)^2 | J, X_J] + 2J\mathbb{E} [T_s - J | X_J] + \mathbb{E} [J^2] \end{aligned}$$

Taking expectations gives (68).

The variance $\mathbb{V}_i[T_s]$ of T_s when starting in state i is given by

$$\begin{aligned}\mathbb{V}_2[T_s] &= \frac{r^3 + \frac{31r^2}{2} + \frac{153r}{2} + 81}{(2r+1)(r+6)(2r^2+13r+9)} + \frac{1}{2} - \frac{1}{4}(1+h(2))^2 \\ \mathbb{V}_1[T_s] &= \frac{r+9}{(r+6)(2r^2+13r+9)} + \frac{1}{2} - \frac{1}{4}(1+h(1))^2 \\ \mathbb{V}_0[T_s] &= \frac{r+8}{(r+6)(2r^2+13r+9)} + \frac{1}{2} - \frac{1}{4}(1+h(0))^2\end{aligned}$$

Hence, $\lim_{r \rightarrow \infty} \mathbb{V}_i[T_s] = 1/4$ for $i \in \{2, 1, 0\}$, and

$$\begin{aligned}\lim_{r \rightarrow 0} \mathbb{V}_2[T_s] &= 1 \\ \lim_{r \rightarrow 0} \mathbb{V}_1[T_s] &= 2/9 \\ \lim_{r \rightarrow 0} \mathbb{V}_0[T_s] &= 89/324\end{aligned}$$

Denote by T_l the time until coalescence has occurred at both loci. The marginal coalescence times are exponential with rate 1, when excluding large offspring numbers. Solving the recursions

$$\begin{aligned}\mathbb{E}_2[T_l] &= (1 + 2r\mathbb{E}_1[T_l]) / (1 + 2r) \\ \mathbb{E}_1[T_l] &= (1 + \mathbb{E}_2[T_l] + r\mathbb{E}_0[T_l] + 2) / (r + 3) \\ \mathbb{E}_0[T_l] &= (1 + 4\mathbb{E}_1[T_l] + 2) / 6\end{aligned}$$

yields

$$\begin{aligned}\mathbb{E}[T_l^{(2)}] &= \frac{3}{2} - \frac{r+9}{2(2r^2+13r+9)} = \frac{1}{2}(3 - h(2)) \\ \mathbb{E}[T_l^{(1)}] &= \frac{3}{2} - \frac{3}{2(2r^2+13r+9)} = \frac{1}{2}(3 - h(1)) \\ \mathbb{E}[T_l^{(0)}] &= \frac{3}{2} - \frac{1}{2r^2+13r+9} = \frac{1}{2}(3 - h(0))\end{aligned}$$

Applying the recursions (68) yields the variances $\mathbb{V}_i[T_l]$;

$$\begin{aligned}\mathbb{V}_2[T_l] &= \frac{2r^3 + \frac{111r^2}{4} + \frac{171r}{2} - \frac{81}{4}}{(2r^2+13r+9)^2} + \frac{5}{4} \\ \mathbb{V}_1[T_l] &= \frac{4r^2 + 17r - \frac{45}{4}}{(2r^2+13r+9)^2} + \frac{5}{4} \\ \mathbb{V}_0[T_l] &= \frac{2r^2 + 7r - 10}{(2r^2+13r+9)^2} + \frac{5}{4}\end{aligned}$$

with $\lim_{r \rightarrow \infty} \mathbb{V}_i[T_l] = 5/4$ for $i \in \{0, 1, 2\}$, and

$$\begin{aligned}\lim_{r \rightarrow 0} \mathbb{V}_2[T_l] &= 1, \\ \lim_{r \rightarrow 0} \mathbb{V}_1[T_l] &= 10/9, \\ \lim_{r \rightarrow 0} \mathbb{V}_0[T_l] &= 365/324.\end{aligned}$$

Now we admit large offspring numbers, take $\varepsilon_N = c/N^2$, and $r_N = r/N$. Ignoring the labelling of the chromosomes, the limit process has three ‘effective’ sample states, depending on the number of double-marked chromosomes $(\vdash\vdash)$. Denote the three sample states by $\binom{\vdash\vdash}{\vdash\vdash}$, $(\vdash\vdash)\binom{\vdash\vdash}{\vdash\vdash}$, and $\binom{\vdash\vdash}{\vdash\vdash}\binom{\vdash\vdash}{\vdash\vdash}$, in which \vdash and \dashv denote single-marked chromosomes. The states of the limit process are composed of single-marked individuals only, and are therefore the same as those of the haploid Wright-Fisher process. By $\bullet\text{---}$ denote a chromosome carrying a common ancestor at one locus, and $(\bullet\text{---}\bullet)$ denotes the absorbing states. The transition rates are summarized in the following table:

	$\binom{\vdash\vdash}{\vdash\vdash}$	$(\vdash\vdash)\binom{\vdash\vdash}{\vdash\vdash}$	$\binom{\vdash\vdash}{\vdash\vdash}\binom{\vdash\vdash}{\vdash\vdash}$	$(\bullet\text{---})\binom{\vdash\vdash}{\vdash\vdash}$	$(\bullet\text{---})(\dashv\vdash)$	$(\bullet\text{---}\bullet)$
$\binom{\vdash\vdash}{\vdash\vdash}$		$2r$				$1 + c\frac{\psi^2}{4}$
$(\vdash\vdash)\binom{\vdash\vdash}{\vdash\vdash}$	$1 + c\frac{\psi^2}{4}(1 - \frac{\psi}{4})$		r		$2 + c\frac{\psi^2}{2}(1 - \frac{\psi}{4})$	$c\frac{\psi^3}{16}$
$\binom{\vdash\vdash}{\vdash\vdash}\binom{\vdash\vdash}{\vdash\vdash}$	$c\frac{3\psi^4}{32}$	$4 + c\left(\psi^2 - \frac{\psi^3}{2} - \frac{\psi^4}{8}\right)$		$2 + c\left(\frac{\psi^2}{2} - \frac{\psi^3}{4} - \frac{\psi^4}{16}\right)$	$c\frac{\psi^3}{4}\left(1 - \frac{\psi}{4}\right)$	$c\frac{\psi^4}{16}$
$(\bullet\text{---})\binom{\vdash\vdash}{\vdash\vdash}$					$2 + c\frac{\psi^2}{2}\left(1 - \frac{\psi}{4}\right)$	$1 + c\frac{\psi^2}{4}$
$(\bullet\text{---})(\dashv\vdash)$				r		$1 + c\frac{\psi^2}{4}$

By way of example, the rate of the transition from 1 to 2 by coalescence of the chromosomes \vdash and \dashv is $1 + cC_{3;2;1}$, the transition rate from 0 to 1 is $4(1 + cC_{4;2;2})$, and the transition rate from 0 to the absorbing state $((\bullet\text{---}\bullet)$ or $(\bullet\text{---})(\dashv\text{---}\bullet))$ is $c(C_{4;4;0} + C_{4;2;2;0})$.

As before, let $h(i)$ denote the probability the two loci coalesce at the same time. One obtains

limit results

$$\begin{aligned}
\lim_{r \rightarrow \infty} h(i) &= \frac{c\psi^4}{32+8c\psi^2-c\psi^4}, \quad i \in \{0, 1, 2\} \\
\lim_{c \rightarrow \infty} h(2) &= 1 \\
\lim_{c \rightarrow \infty} h(1) &= \frac{2}{6-\psi} \\
\lim_{c \rightarrow \infty} h(0) &= \frac{\frac{56}{3}\psi^2 - 272\psi + 544}{(\psi-6)(3\psi^2+16\psi-48)} - \frac{5}{3}
\end{aligned} \tag{69}$$

The first equation in (69) tells us that the loci remain correlated due to multiple mergers even when they are far apart on a chromosome. When the recombination rate r is quite small, one obtains

$$\begin{aligned}
\lim_{r \rightarrow 0} h(2) &= 1 \\
\lim_{r \rightarrow 0} h(1) &= \frac{2(c\psi^2+4)}{-c\psi^3+6c\psi^2+24} \\
\lim_{r \rightarrow 0} h(0) &= \frac{1}{3} \left(\frac{8c\psi^2+32}{-c\psi^3+6c\psi^2+24} + \frac{-80c\psi^3+208c\psi^2+832}{-3c\psi^4-16c\psi^3+48c\psi^2+192} - 5 \right)
\end{aligned} \tag{70}$$

Let $\mathbb{E}_i[T_s]$, as before, denote the time until coalescence at either loci, starting from state i . Admitting large offspring numbers, one obtains

$$\begin{aligned}
\lim_{r \rightarrow \infty} \mathbb{E}_i[T_s] &= \frac{16}{32+8c\psi^2-c\psi^4}, \quad i \in \{0, 1, 2\}, \\
\lim_{c \rightarrow \infty} \mathbb{E}_i[T_s] &= 0, \quad i \in \{0, 1, 2\}, \\
\lim_{r \rightarrow 0} \mathbb{E}_2[T_s] &= \frac{4}{c\psi^2+4} \\
\lim_{r \rightarrow 0} \mathbb{E}_1[T_s] &= \frac{c(16\psi^2-2\psi^3)+64}{-c^2\psi^5+6c^2\psi^4-4c\psi^3+48c\psi^2+96} \\
\lim_{r \rightarrow 0} \mathbb{E}_0[T_s] &= \frac{16}{3(c(6\psi^2-\psi^3)+24)} - \frac{4(\psi-8)}{(3\psi+16)(c\psi^2+4)} - \frac{32(39\psi-32)}{3(c(3\psi^4+16\psi^3-48\psi^2)-192)(3\psi+16)}
\end{aligned}$$

Let $\mathbb{E}_i[T_l]$, as before, denote the expected value of the time T_l until coalescence has occurred at both

loci, when starting from state i . Admitting large offspring numbers, one obtains the limits

$$\begin{aligned}\lim_{r \rightarrow \infty} \mathbb{E}_i[T_i] &= \frac{c(48\psi^2 - 8\psi^4) + 192}{(c\psi^2 + 4)(-c\psi^4 + 8c\psi^2 + 32)}, \quad i \in \{0, 1, 2\}, \\ \lim_{c \rightarrow \infty} \mathbb{E}_i[T_i] &= 0, \quad i \in \{0, 1, 2\}, \\ \lim_{r \rightarrow 0} \mathbb{E}_2[T_i] &= \frac{4}{c\psi^2 + 4} \\ \lim_{r \rightarrow 0} \mathbb{E}_1[T_i] &= \frac{c(32\psi^2 - 6\psi^3) + 128}{-c^2\psi^5 + 6c^2\psi^4 - 4c\psi^3 + 48c\psi^2 + 96} \\ \lim_{r \rightarrow 0} \mathbb{E}_0[T_i] &= \frac{(28\psi^7 - 56\psi^6 - 800\psi^5 + 1600\psi^4)c^2 + (-608\psi^4 - 3200\psi^3 + 12800\psi^2)c + 25600}{a}\end{aligned}$$

in which

$$\begin{aligned}a &= 3c^3\psi^9 - 2c^3\psi^8 - 144c^3\psi^7 + 288c^3\psi^6 + 12c^2\psi^7 - 80c^2\psi^6 - 1152c^2\psi^5 \\ &\quad + 3456c^2\psi^4 - 288c\psi^4 - 2304c\psi^3 + 13824c\psi^2 + 18432\end{aligned}$$

Considering the variance $\mathbb{V}_i[T_s]$ of the time T_s when starting from state $i \in \{0, 1, 2\}$, and admitting large offspring numbers, one obtains

$$\begin{aligned}\lim_{r \rightarrow \infty} \mathbb{V}_i[T_s] &= \frac{256}{(c(8\psi^2 - \psi^4) + 32)^2}, \quad i \in \{0, 1, 2\}, \\ \lim_{c \rightarrow \infty} \mathbb{V}_2[T_s] &= 0, \quad i \in \{0, 1, 2\}, \\ \lim_{r \rightarrow 0} \mathbb{V}_2[T_s] &= \frac{16}{(c\psi^2 + 4)^2} \\ \lim_{r \rightarrow 0} \mathbb{V}_1[T_s] &= \frac{(12\psi^6 - 128\psi^5 + 384\psi^4)c^2 + (3072\psi^2 - 512\psi^3)c + 6144}{(c\psi^2 + 4)^2(-c\psi^3 + 6c\psi^2 + 24)^2}\end{aligned}$$

Correlations in coalescence times have been employed to quantify linkage disequilibrium (LD) (MCVEAN, 2002), in which LD is quantified as the square of the correlation coefficient of types at two loci (HILL and ROBERSON, 1968). A description of how one can quantify linkage disequilibrium as the square of the correlation coefficient of types at two loci can be found in HARTL and CLARK (1989). Assuming a very small mutation rate, MCVEAN (2002) related \mathfrak{D} to covariances in coalescence times. Writing $\text{Cov}_i(T_1, T_2)$ as the covariance of T_1 and T_2 when starting from state

$i \in \{0, 1, 2\}$, McVEAN (2002) obtained

$$\begin{aligned}\mathfrak{D} &= \frac{\text{Cov}_2 [T_1, T_2] - 2\text{Cov}_1 [T_1, T_2] + \text{Cov}_0 [T_1, T_2]}{(\mathbb{E}[T_1])^2 + \text{Cov}_0 [T_1, T_2]} \\ &= 1 + \frac{\mathbb{E}_2 [T_1 T_2] - 2\mathbb{E}_1 [T_1 T_2]}{\mathbb{E}_0 [T_1 T_2]}\end{aligned}$$

in which T_1 and T_2 denote the times until coalescence at the two loci, respectively, and the covariances are conditional on the sample configurations, as indicated. Following e.g. DURRETT (2002) one can obtain the covariances under any population model. Under our population model, $\mathfrak{D} = \mathfrak{D}_1/\mathfrak{D}_2$, in which

$$\begin{aligned}\mathfrak{D}_1 &= 640c\psi^2 - 224c\psi^3 + 32c\psi^4 + 80c^2\psi^4 - 56c^2\psi^5 + 16c^2\psi^6 - c^2\psi^7 \\ &\quad + r(16c\psi^4 - 32c\psi^3 + 64c\psi^2 + 256) + 1280, \\ \mathfrak{D}_2 &= 1408c\psi^2 - 352c\psi^3 + 8c\psi^4 + 512r^2 + 176c^2\psi^4 - 88c^2\psi^5 + 10c^2\psi^6 - c^2\psi^7 \\ &\quad + r(8c\psi^4 - 288c\psi^3 + 832c\psi^2 + 3328) + 2816.\end{aligned}$$

One obtains the limit results

$$\begin{aligned}\lim_{r \rightarrow \infty} \mathfrak{D} &= 0, \\ \lim_{c \rightarrow \infty} \mathfrak{D} &= \frac{\psi^3 - 16\psi^2 + 56\psi - 80}{\psi^3 - 10\psi^2 + 88\psi - 176}.\end{aligned}$$

1.6 Correlations in coalescence times for random ψ

In this section we consider the simple example of the probability measure F , evoked in relation to a random offspring distribution, taking the beta distribution with parameters ϑ and γ . The

following transition rates for a sample of size two at two loci are obtained:

	$\begin{pmatrix} (-) \\ (-) \end{pmatrix}$	$\begin{pmatrix} (-) \\ (-) \end{pmatrix} \begin{pmatrix} (-) \\ (-) \end{pmatrix}$	$\begin{pmatrix} (-) \\ (-) \end{pmatrix} \begin{pmatrix} (-) \\ (-) \end{pmatrix}$	$\begin{pmatrix} (-) \\ (-) \end{pmatrix} \begin{pmatrix} (-) \\ (-) \end{pmatrix}$	$\begin{pmatrix} (-) \\ (-) \end{pmatrix} \begin{pmatrix} (-) \\ (-) \end{pmatrix}$	$\begin{pmatrix} (-) \\ (-) \end{pmatrix} \begin{pmatrix} (-) \\ (-) \end{pmatrix}$
$\begin{pmatrix} (-) \\ (-) \end{pmatrix}$		$2r$				1
$\begin{pmatrix} (-) \\ (-) \end{pmatrix} \begin{pmatrix} (-) \\ (-) \end{pmatrix}$	$\frac{\gamma+3\vartheta/4}{\vartheta+\gamma}$		r		$2\frac{\gamma+3\vartheta/4}{\vartheta+\gamma}$	$\frac{\vartheta}{4(\vartheta+\gamma)}$
$\begin{pmatrix} (-) \\ (-) \end{pmatrix} \begin{pmatrix} (-) \\ (-) \end{pmatrix}$	$\frac{3}{8} \frac{(1+\vartheta)\vartheta}{(1+\vartheta+\gamma)(\vartheta+\gamma)}$	$\frac{4(1+\gamma)\gamma+3\vartheta\gamma+\frac{3}{2}(1+\vartheta)\vartheta}{(1+\vartheta+\gamma)(\vartheta+\gamma)}$		$\frac{2(1+\gamma)\gamma+\frac{3}{2}\vartheta\gamma+\frac{3}{4}(1+\vartheta)\vartheta}{(1+\vartheta+\gamma)(\vartheta+\gamma)}$	$\frac{\vartheta\gamma+\frac{3}{4}(1+\vartheta)\vartheta}{(1+\vartheta+\gamma)(\vartheta+\gamma)}$	$\frac{(\vartheta+1)\vartheta}{4(\vartheta+\gamma+1)(\vartheta+\gamma)}$
$\begin{pmatrix} (-) \\ (-) \end{pmatrix} \begin{pmatrix} (-) \\ (-) \end{pmatrix}$					$2\frac{\gamma+3\vartheta/4}{\vartheta+\gamma}$	1
$\begin{pmatrix} (-) \\ (-) \end{pmatrix} \begin{pmatrix} (-) \\ (-) \end{pmatrix}$				r		1

As before, the transition rates given above can be employed to derive correlations in coalescence times. Here we only consider the probability $h(i)$. One obtains $\lim_{\vartheta \rightarrow 0} h(i) = \lim_{\gamma \rightarrow \infty} h(i)$ and the limit results are those obtained from the usual ARG (67).

1.7 Variance of pairwise differences The variance of pairwise differences between DNA sequences has been employed to estimate recombination rates in low offspring number populations (WAKELEY, 1997). Let the random variable K_{ij} denote the number of differences between sequences i and j , with $K_{ii} = 0$. The average number π of pairwise differences for n sequences is

$$\pi = \frac{2}{n(n-1)} \sum_{i < j} K_{ij}$$

Under the infinitely many sites mutation model, $\mathbb{E}[\pi] = \theta\mathbb{E}[T]$, in which T is the time until coalescence of two sequences. Under our model, $\mathbb{E}[T] = 1/(1 + c\psi^2/4)$. Define the variance S_π^2 of pairwise differences as

$$S_\pi^2 = \frac{2}{n(n-1)} \sum_{i < j} (K_{ij} - \pi)^2$$

To obtain an estimate of the recombination rate, one needs to compute the expected value $\mathbb{E} [S_\pi^2]$,

$$\mathbb{E} [S_\pi^2] = \frac{2}{n(n-1)} \sum_{i < j} \mathbb{E} [(K_{ij} - \pi)^2] = \mathbb{E} [(K_{12} - \pi)^2].$$

Thus, it suffices to consider $\mathbb{E} [(K_{12} - \pi)^2]$. Expanding, one obtains

$$\begin{aligned} \mathbb{E} [(K_{12} - \pi)^2] &= \mathbb{E} \left[\left(\frac{2}{n(n-1)} \sum_{i < j} (K_{12} - K_{ij}) \right)^2 \right] \\ &= \frac{4}{n^2(n-1)^2} \sum_{i < j} \sum_{\hat{i} < \hat{j}} \mathbb{E} [(K_{12} - K_{ij})(K_{12} - K_{\hat{i}\hat{j}})]. \end{aligned}$$

Define the event $A_{ij}^{(\ell)}$ by

$$A_{ij}^{(\ell)} := \{\text{sequences } i \text{ and } j \text{ differ at locus } \ell\}.$$

Assuming each sequence consists of L loci, and $1_{A_{ij}^{(\cdot)}}$ are indicator functions,

$$K_{12} - K_{ij} = \sum_{\ell=1}^L \left(1_{A_{12}^{(\ell)}} - 1_{A_{ij}^{(\ell)}} \right)$$

yielding, in case $i = i' = 1$, and $j = \hat{j} = 3$,

$$\begin{aligned} \mathbb{E} [(K_{12} - K_{13})^2] &= \sum_{\ell=1}^L \sum_{\hat{\ell}=1}^L \mathbb{E} \left[\left(1_{A_{12}^{(\ell)}} - 1_{A_{13}^{(\ell)}} \right) \left(1_{A_{12}^{(\hat{\ell})}} - 1_{A_{13}^{(\hat{\ell})}} \right) \right] \\ &= 2 \sum_{\ell=1}^L \sum_{\hat{\ell}=1}^L \mathbb{P} \left(A_{12}^{(\ell)} \cap A_{12}^{(\hat{\ell})} \right) - \mathbb{P} \left(A_{12}^{(\ell)} \cap A_{13}^{(\hat{\ell})} \right). \end{aligned}$$

In general,

$$\begin{aligned}
& \mathbb{E} [(K_{12} - K_{ij})(K_{12} - K_{ij})] \\
&= \sum_{\ell=1}^L \sum_{\hat{\ell}=1}^L \mathbb{E} \left[\left(1_{A_{12}^{(\ell)}} - 1_{A_{ij}^{(\ell)}} \right) \left(1_{A_{12}^{(\hat{\ell})}} - 1_{A_{ij}^{(\hat{\ell})}} \right) \right] \\
&= \sum_{\ell=1}^L \sum_{\hat{\ell}=1}^L \mathbb{P} \left(A_{12}^{(\ell)} \cap A_{12}^{(\hat{\ell})} \right) - \mathbb{P} \left(A_{12}^{(\ell)} \cap A_{ij}^{(\hat{\ell})} \right) - \mathbb{P} \left(A_{12}^{(\hat{\ell})} \cap A_{ij}^{(\ell)} \right) + \mathbb{P} \left(A_{ij}^{(\ell)} \cap A_{ij}^{(\hat{\ell})} \right).
\end{aligned} \tag{71}$$

Now consider the probability $\mathbb{P}(A_{12}^{(\ell)} \cap A_{12}^{(\hat{\ell})})$ of the event that sequences 1 and 2 differ at both loci ℓ and $\hat{\ell}$. Admitting mutation introduces two new states, namely the states $\binom{+}{-}$ and $\binom{-}{+}$. Define

$$g(\mathfrak{S}) := \mathbb{P}(\text{both loci separated by mutation, starting from state } \mathfrak{S})$$

Thus, $\mathbb{P} \left(A_{12}^{(\ell)} \cap A_{12}^{(\hat{\ell})} \right) = g(2)$, $\mathbb{P} \left(A_{12}^{(\ell)} \cap A_{13}^{(\hat{\ell})} \right) = g(1)$, and $\mathbb{P} \left(A_{12}^{(\ell)} \cap A_{34}^{(\hat{\ell})} \right) = g(0)$, for $\ell \neq \hat{\ell}$.

Now,

$$\begin{aligned}
g(2) &= \frac{\theta_1 g(-1) + \theta_2 g(-2) + 2r g(1)}{\theta_1 + \theta_2 + 1 + c \frac{\psi^2}{4} + 2r} \\
g(-1) &= \frac{\theta_2}{\theta_2 + 1 + c \frac{\psi^2}{4}} \\
g(-2) &= \frac{\theta_1}{\theta_1 + 1 + c \frac{\psi^2}{4}} \\
g(1) &= \frac{\theta_1 g(-1) + \theta_2 g(-2) + r g(0) + (1 + c\psi^2/4) g(2)}{\theta_1 + \theta_2 + r + 3 + 3c \frac{\psi^2}{4} (1 - \frac{\psi}{4}) + c \frac{\psi^3}{16}} \\
g(0) &= \frac{\theta_1 g(-1) + \theta_2 g(-2) + c \frac{3\psi^4}{32} g(2) + \left(c \left(\psi^2 - \frac{\psi^3}{2} - \frac{\psi^4}{8} \right) + 4 \right) g(1)}{c \frac{3\psi^4}{32} + c \left(\psi^2 - \frac{\psi^3}{2} - \frac{\psi^4}{8} \right) + c \left(\frac{\psi^2}{2} - \frac{\psi^3}{4} - \frac{\psi^4}{16} \right) + 6 + c \frac{\psi^3}{4} \left(1 - \frac{\psi}{4} \right) + c \frac{\psi^4}{16} + \theta_1 + \theta_2}
\end{aligned}$$

In view of expression (71), one obtains

$$\begin{aligned}
\mathbb{P}\left(A_{12}^{(\ell)} \cap A_{12}^{(\ell)}\right) &= \mathbb{P}\left(A_{12}^{(\ell)}\right) = \frac{\theta_\ell}{\theta_\ell + 1 + c\psi^2/4}, \\
\mathbb{P}\left(A_{12}^{(\ell)} \cap A_{13}^{(\ell)}\right) &= \frac{\theta_\ell}{\frac{3\theta_\ell}{2} + \lambda_3} + \frac{\lambda_2}{\frac{3\theta_\ell}{2} + \lambda_3} \frac{\theta_\ell}{\theta_\ell + \lambda_2}, \\
\mathbb{P}\left(A_{12}^{(\ell)} \cap A_{34}^{(\ell)}\right) &= \frac{2\theta_\ell}{2\theta_\ell + \lambda_4} \frac{\theta_\ell}{2\theta_\ell + \lambda_4} + \frac{\lambda_{4;2}}{2\theta_\ell + \lambda_4} \left(\frac{\theta_\ell/2}{\frac{3\theta_\ell}{2} + \lambda_3} + \left(\frac{\theta_\ell/2}{\frac{3\theta_\ell}{2} + \lambda_3} \right)^2 \right).
\end{aligned} \tag{72}$$

The event $A_{12}^{(\ell)} \cap A_{34}^{(\ell)}$ (72) occurs if the first two events in the history of the four sequences are mutations on appropriate ancestral lineages, or if lineages labelled 2 and 3 coalesce, followed by appropriately-placed mutations.

Table 4: Estimates \bar{R}_i of the expected values $E[R_i]$ of the ratios $R_i := L_i/L$ for $1 \leq i \leq 4$ at one marginal locus, along with estimates \hat{R}_i of the standard deviations of R_i . Estimates are obtained from 10^5 simulated gene genealogies.

ψ	c	n	\bar{R}_1	\bar{R}_2	\bar{R}_3	\bar{R}_4	\hat{R}_1	\hat{R}_2	\hat{R}_3	\hat{R}_4
-	0	6	0.466	0.219	0.138	0.100	0.183	0.167	0.198	0.124
		10	0.378	0.180	0.117	0.085	0.156	0.132	0.120	0.110
		20	0.300	0.146	0.096	0.070	0.119	0.097	0.088	0.081
		50	0.235	0.116	0.077	0.057	0.080	0.063	0.058	0.055
0.005	1	6	0.466	0.219	0.138	0.100	0.183	0.167	0.198	0.124
		10	0.377	0.181	0.117	0.085	0.156	0.133	0.120	0.111
		20	0.299	0.146	0.095	0.071	0.118	0.097	0.088	0.082
		50	0.234	0.116	0.076	0.057	0.080	0.064	0.057	0.054
	1000	6	0.467	0.219	0.137	0.100	0.182	0.167	0.198	0.124
		10	0.377	0.181	0.117	0.085	0.156	0.133	0.120	0.110
		20	0.299	0.146	0.095	0.071	0.119	0.097	0.088	0.082
		50	0.235	0.116	0.077	0.057	0.080	0.064	0.058	0.054
0.5	1	6	0.468	0.217	0.138	0.099	0.184	0.166	0.199	0.124
		10	0.381	0.179	0.115	0.085	0.157	0.132	0.120	0.110
		20	0.304	0.145	0.095	0.070	0.120	0.097	0.088	0.081
		50	0.242	0.117	0.077	0.056	0.081	0.064	0.058	0.054
	1000	6	0.541	0.173	0.116	0.089	0.184	0.152	0.177	0.116
		10	0.566	0.117	0.078	0.058	0.159	0.101	0.090	0.082
		20	0.743	0.101	0.035	0.022	0.084	0.053	0.033	0.027
		50	0.576	0.195	0.089	0.046	0.058	0.051	0.037	0.026

Table 5: Estimates of the correlation $\text{cor}(X^{(1)}, Y^{(2)})$ between $X^{(1)}$ and $Y^{(2)}$, where $X^{(1)}$ represents a statistic for locus 1, and $Y^{(2)}$ for locus 2, as follows: the time T until most recent common ancestor at a locus; L the total length of the gene genealogy at a locus, and $R_i := L_i/L$, in which L_i denotes the total length of branches ancestral to i sequences. Estimates are based on 10^5 simulated ancestral recombination graphs each for a sample of size 50.

c	ψ	r	$\text{cor}(T^{(1)}, T^{(2)})$	$\text{cor}(L^{(1)}, L^{(2)})$	$\text{cor}(L_1^{(1)}, L_1^{(2)})$	$\text{cor}(L_2^{(1)}, L_2^{(2)})$	$\text{cor}(L_3^{(1)}, L_3^{(2)})$	$\text{cor}(L_4^{(1)}, L_4^{(2)})$
0	-	1	0.311	0.418	0.586	0.501	0.434	0.378
		10	0.016	0.058	0.169	0.089	0.047	0.036
1	0.005	1	0.306	0.415	0.588	0.508	0.431	0.380
		10	0.015	0.055	0.171	0.090	0.049	0.034
1000	0.005	1	0.308	0.419	0.585	0.509	0.438	0.376
		10	0.013	0.051	0.168	0.093	0.052	0.030
1	0.5	1	0.328	0.447	0.601	0.516	0.449	0.389
1		10	0.024	0.085	0.193	0.107	0.064	0.036
1000		1	0.982	0.995	0.976	0.950	0.918	0.879
		10	0.924	0.947	0.763	0.623	0.503	0.396
c	ψ	r	$\text{cor}(L_1^{(1)}, L_2^{(2)})$	$\text{cor}(L_1^{(1)}, L_3^{(2)})$	$\text{cor}(L_1^{(1)}, L_4^{(2)})$	$\text{cor}(L_2^{(1)}, L_3^{(2)})$	$\text{cor}(L_2^{(1)}, L_4^{(2)})$	$\text{cor}(L_3^{(1)}, L_4^{(2)})$
0	-	1	-0.031	-0.031	-0.021	-0.005	-0.018	0.009
		10	0.005	-0.006	-0.001	0.012	0.005	0.013
1	0.005	1	-0.035	-0.025	-0.021	-0.001	-0.019	0.009
		10	0.000	-0.002	0.008	0.009	0.005	0.014
1000	0.005	1	-0.036	-0.029	-0.021	-0.006	-0.018	0.010
		10	-0.002	-0.003	0.003	0.014	0.004	0.005
1	0.5	1	-0.022	-0.014	-0.007	0.004	-0.004	0.023
		10	0.009	0.006	0.010	0.022	0.014	0.025
1000		1	0.326	0.314	0.305	0.238	0.218	0.176
		10	0.311	0.284	0.266	0.289	0.239	0.262

Table 6: Estimates of the correlation $\text{cor}(X^{(1)}, Y^{(2)})$ between $X^{(1)}$ and $Y^{(2)}$, where $X^{(1)}$ represents a statistic for locus 1, and $Y^{(2)}$ for locus 2, as follows: the time T until most recent common ancestor at a locus; L the total length of the gene genealogy at a locus, and $R_i := L_i/L$, in which L_i denotes the total length of branches ancestral to i sequences. Estimates are based on 10^5 simulated ancestral recombination graphs each for a sample of size 50.

c	ψ	r	$\text{cor}(R_1^{(1)}, R_1^{(2)})$	$\text{cor}(R_2^{(1)}, R_2^{(2)})$	$\text{cor}(R_3^{(1)}, R_3^{(2)})$	$\text{cor}(R_4^{(1)}, R_4^{(2)})$
0	-	1	0.570	0.548	0.486	0.431
		10	0.116	0.089	0.052	0.042
1	0.005	1	0.566	0.552	0.487	0.435
		10	0.115	0.091	0.054	0.035
1000	0.005	1	0.570	0.551	0.491	0.434
		10	0.115	0.095	0.059	0.031
1	0.5	1	0.583	0.557	0.504	0.447
		10	0.135	0.102	0.063	0.038
1000	0.5	1	0.955	0.927	0.900	0.866
		10	0.679	0.469	0.384	0.304

c	ψ	r	$\text{cor}(R_1^{(1)}, R_2^{(2)})$	$\text{cor}(R_1^{(1)}, R_3^{(2)})$	$\text{cor}(R_1^{(1)}, R_4^{(2)})$	$\text{cor}(R_2^{(1)}, R_3^{(2)})$	$\text{cor}(R_2^{(1)}, R_4^{(2)})$	$\text{cor}(R_3^{(1)}, R_4^{(2)})$
0	-	1	-0.023	-0.040	-0.042	-0.026	-0.042	-0.014
		10	-0.022	-0.023	-0.020	0.003	-0.005	0.005
1	0.005	1	-0.024	-0.038	-0.042	-0.023	-0.046	-0.014
		10	-0.027	-0.018	-0.015	0.001	-0.007	0.011
1000	0.005	1	-0.028	-0.038	-0.038	-0.031	-0.043	-0.012
		10	-0.030	-0.024	-0.016	0.003	-0.008	-0.001
1	0.5	1	-0.023	-0.035	-0.035	-0.028	-0.034	
1	0.5	10	-0.029	-0.023	-0.015	0.004	0.000	
1000	1	1	-0.622	-0.348	-0.112	-0.100	-0.038	-0.016
		10	-0.330	-0.255	-0.135	0.009	0.004	0.096

Figure 2: The probabilities $h(2)$, $h(1)$, and $h(0)$ as functions of ψ (lines) for different values of r and c . Values of $h(\cdot)$ obtained from the usual Moran model are shown for reference (symbols).

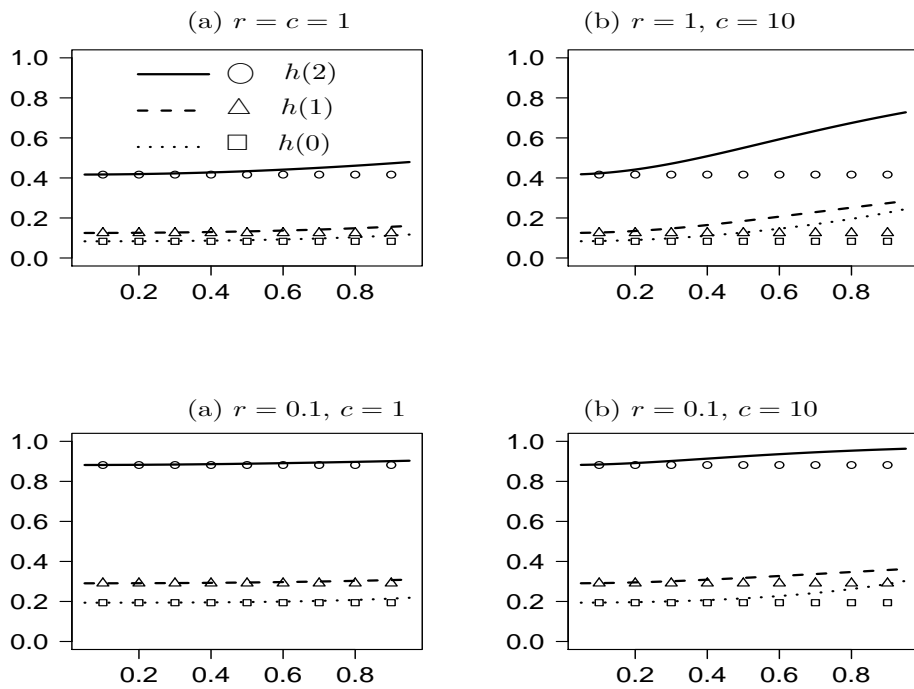


Figure 3: The expected time $\mathbb{E}[T_s^{(i)}]$ as a function of ψ for different values of c and r . Values of $\mathbb{E}[T_s^{(i)}]$ associated with the case $c = 0$ are shown for reference (symbols).

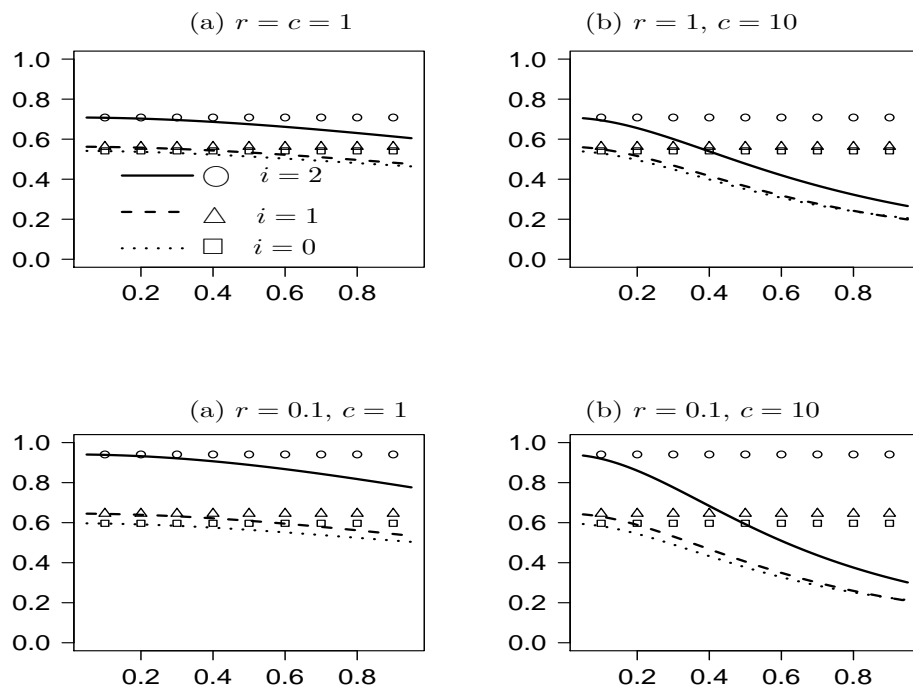


Figure 4: The expected time $\mathbb{E}[T_l^{(i)}]$ as a function of ψ for different values of c and r . For explanation of symbols, see Figure 3.

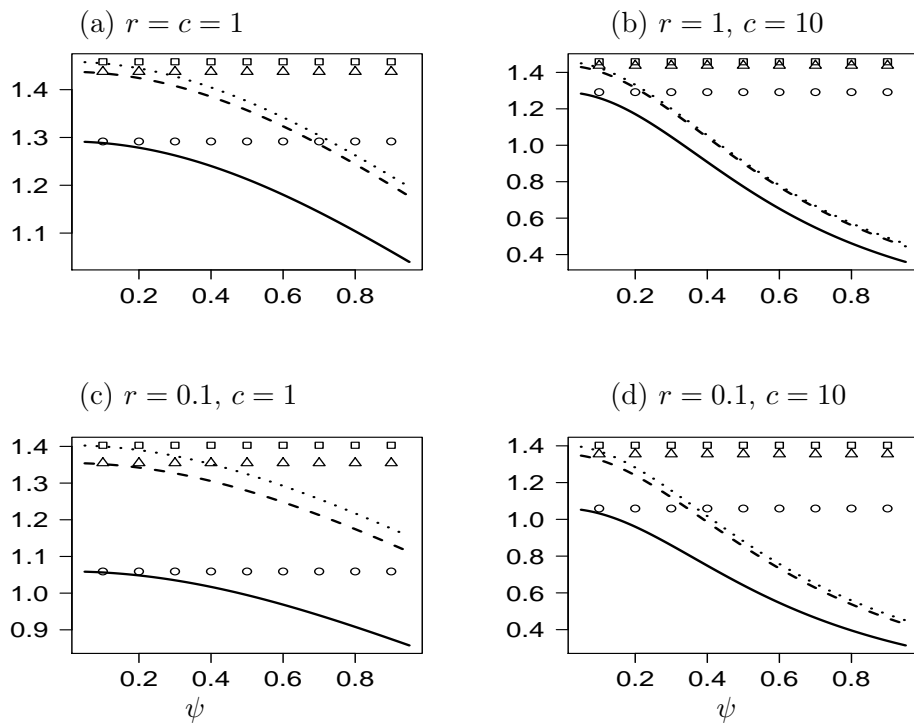


Figure 5: Correlation of the time to coalescence at two loci as a function of ψ , for different values of c and r . For explanation of symbols, see Figure 3.

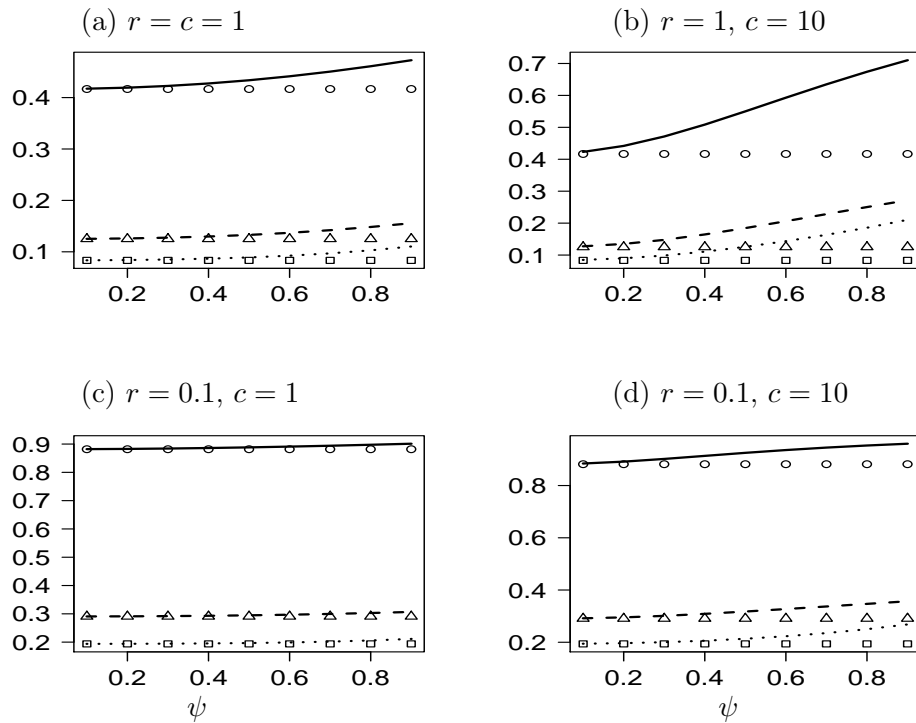


Figure 6: The estimate \mathfrak{D} of the expected value $\mathbb{E}[r^2]$ as a function of ψ for different values of c (see panels), and r . The solid lines represent the value of \mathfrak{D} associated with the usual Wright-Fisher model.

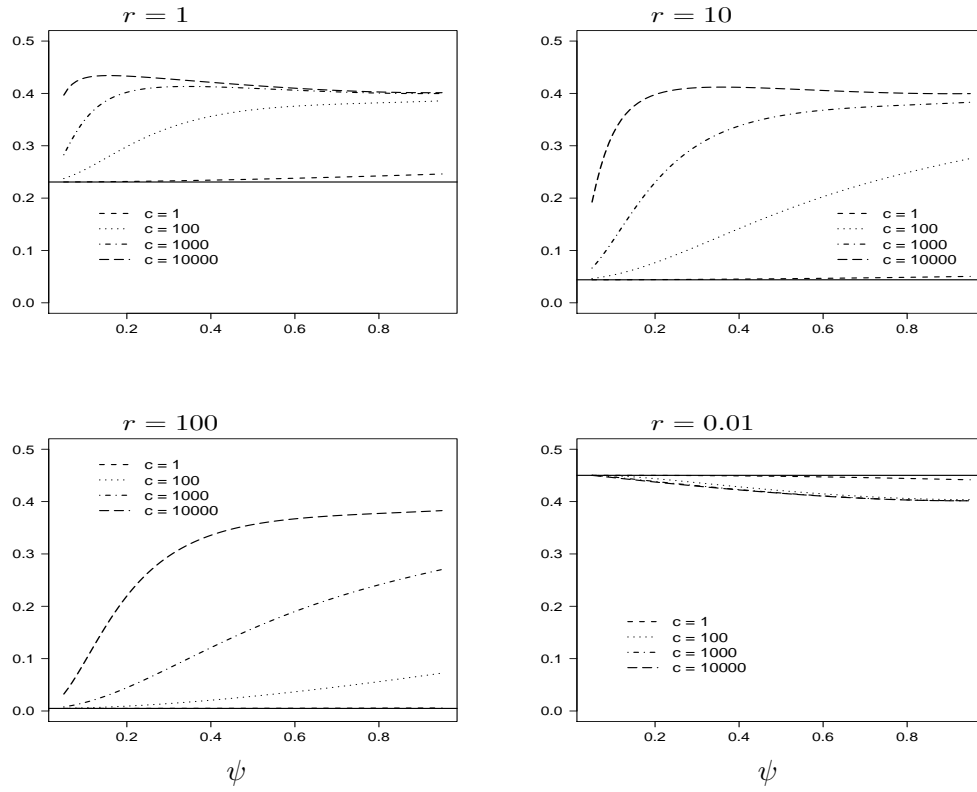


Figure 7: The prediction \mathfrak{D} of linkage disequilibrium obtained from the ARG associated with the Beta(ϑ, γ) dist. The different lines represent different values of γ (upper panels) or ϑ (lower panels). The broken horizontal line represents the prediction obtained from the usual ARG.

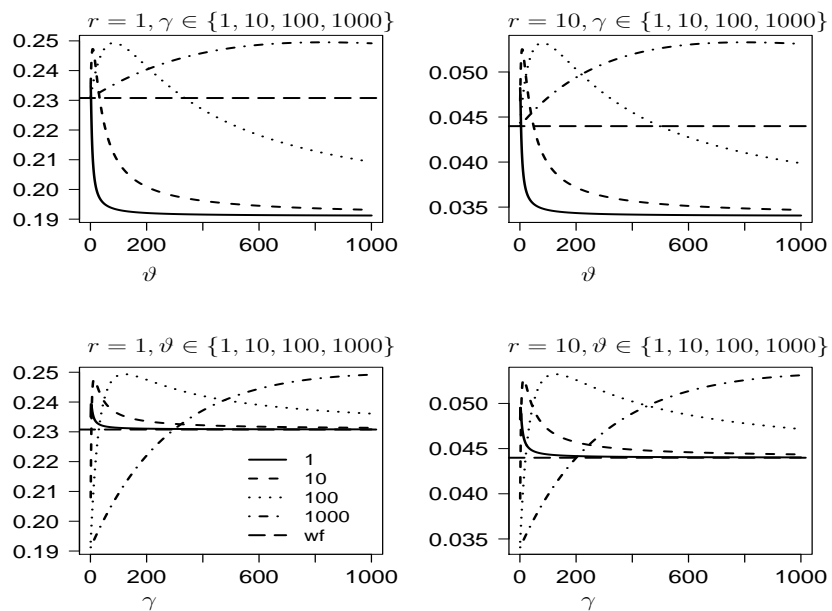


Figure 8: The expected variance of pairwise differences for sample size 50 as a function of the recombination rate r for different values of the parameters c , ψ , and θ as shown.

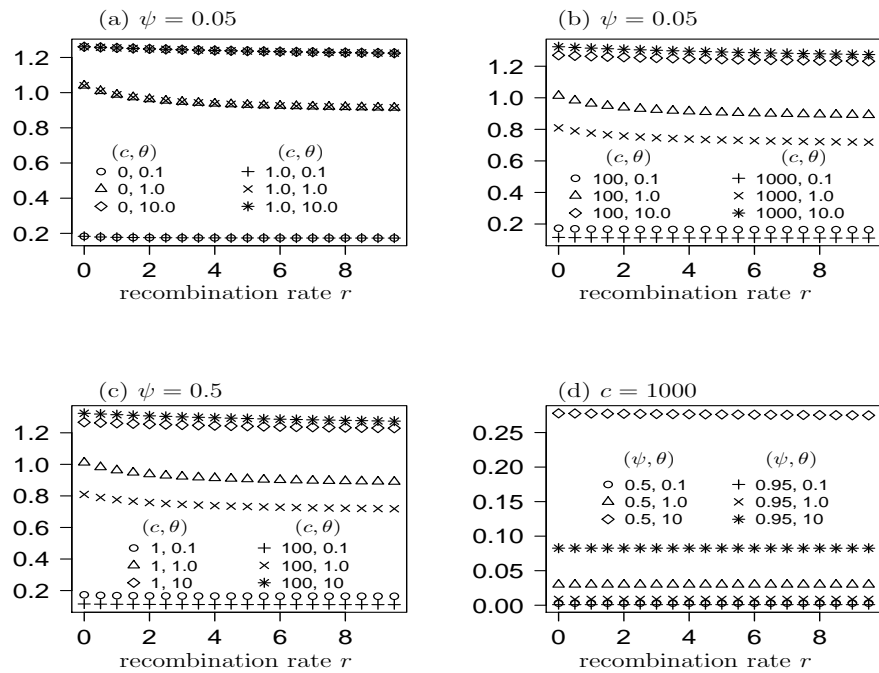


Figure 9: The expected variance of pairwise differences as a function of sample size for different values of the parameters c , ψ , r , and θ as shown.

